MOLECULAR AND CELLULAR BIOLOGY, Mar. 1997, p. 1298–1313 Vol. 17, No. 3
0270-7306/97/$04.00+0

Homologous Segments in Three Subunits of the Guanine Nucleotide Exchange Factor eIF2B Mediate Translational Regulation by Phosphorylation of eIF2

GRAHAM D. PAVITT, WEIMIN YANG, AND ALAN G. HINNEBUSCH*

Laboratory of Eukaryotic Gene Regulation, National Institute of Child Health and Human Development, National Institutes of Health, Bethesda, Maryland 20892

Received 30 August 1996/Returned for modification 29 October 1996/Accepted 20 November 1996

eIF2B is a five-subunit guanine nucleotide exchange factor that is negatively regulated by phosphorylation of the α subunit of its substrate, eIF2, leading to inhibition of translation initiation. To analyze this regulatory mechanism, we have characterized 29 novel mutations in the homologous eIF2B subunits encoded by *GCD2*, *GCD7*, and *GCN3* that reduce or abolish inhibition of eIF2B activity by eIF2 phosphorylated on its α subunit [eIF2(αP)]. Most, if not all, of the mutations decrease sensitivity to eIF2(αP) without excluding GCN3, the nonessential subunit, from eIF2B; thus, all three proteins are critical for regulation of eIF2B by eIF2(αP). The mutations are clustered at both ends of the homologous region of each subunit, within two segments each of approximately 70 amino acids in length. Several mutations alter residues at equivalent positions in two or all three subunits. These results imply that structurally similar segments in GCD2, GCD7, and GCN3 perform related functions in eIF2B regulation. We propose that these segments form a single domain in eIF2B that makes multiple contacts with the α subunit of eIF2, around the phosphorylation site, allowing eIF2B to detect and respond to phosphoserine at residue 51. Most of the eIF2 is phosphorylated in certain mutants, suggesting that these substitutions allow eIF2B to accept phosphorylated eIF2 as a substrate for nucleotide exchange.

The current model for translation initiation proposes that translation initiation factor 2 (eIF2) forms a ternary complex with GTP and charged initiator $tRNA^{Met}$, which binds to 40S ribosomes. After mRNA binding to the ribosome and recognition of the AUG codon by initiator $tRNA^{Met}$, GTP hydrolysis releases an eIF2 · GDP binary complex. For eIF2 to participate in further rounds of initiation, it must be recycled to eIF2 · GTP by the guanine nucleotide exchange factor eIF2B. This recycling of eIF2 · GDP to eIF2 · GTP by eIF2B is inhibited by phosphorylation of eIF2 on its α subunit (eIF2α) at serine 51 (reviewed in references 30 and 44). Three protein kinases, known as HRI, PKR, and GCN2, specifically phosphorylate Ser-51 of eIF2α under different stress conditions (12, 48). HRI is activated in mammalian reticulocytes in response to heme deprivation, whereas PKR (also known as DAI or p68 kinase) is part of the antiviral response and is activated by double-stranded RNA. Both kinases phosphorylate eIF2 to shut off total protein synthesis by complete inhibition of eIF2B.

In the yeast *Saccharomyces cerevisiae*, GCN2 phosphorylates eIF2 in response to starvation for amino acids or purines. The level of eIF2 phosphorylated on its α subunit [eIF2(αP)] produced by moderate starvation in yeast cells is not sufficient to inhibit total protein synthesis; however, it does result in a specific increase in translation of *GCN4* mRNA, encoding a transcriptional activator of amino acid biosynthetic genes (reviewed in reference 23). Thus, translation of *GCN4* is inversely coupled to the concentration of eIF2 · GTP · $tRNA_i^{Met}$ ternary complexes and, therefore, to the catalytic activity of eIF2B. Mutationally activated forms of GCN2 that generate higher levels of eIF2(αP) than are seen in nutrient-deprived cells have been isolated (35, 51), and in these *GCN2^c* mutants, or in yeast cells expressing human PKR or HRI (15), general translation initiation and cellular growth are greatly inhibited.

Strong genetic evidence supports the model that phosphorylation of eIF2α on Ser-51 regulates translation initiation in yeast by inhibiting eIF2B function, just as in mammalian cells. All five subunits of eIF2B, encoded by *GCN3*, *GCD7*, *GCD1*, *GCD2*, and *GCD6* (equivalent to the mammalian polypeptides α to ε, respectively), were first identified genetically as regulators of *GCN4* translation (21). The *GCD* genes encoding eIF2B subunits are essential, and nonlethal mutations in each result in constitutive high-level translation of *GCN4* (Gcd^- phenotype) and reduced cellular growth rates on nutrient-rich media. Presumably, these *gcd* mutations lead to decreased ternary complex concentrations independently of eIF2 phosphorylation by impairing eIF2B structure or catalytic activity. In contrast, the GCN3 subunit of eIF2B is dispensable, and its inactivation impairs only the ability to stimulate *GCN4* translation under starvation conditions (19, 24). This is the same Gcn^- phenotype observed following inactivation of the protein kinase GCN2 or replacement of Ser-51 in eIF2α with nonphosphorylatable alanine (16). Therefore, it was proposed that GCN3 is a regulatory subunit required to mediate the inhibitory effect of eIF2(αP) on eIF2B function (15). It was shown recently that the effects of eIF2 phosphorylation on *GCN4*-specific and general translation initiation are reduced by overproducing all five subunits of eIF2B or, even more effectively, by overexpressing just a four-subunit complex containing the essential subunits GCD7, GCD1, GCD2, and GCD6 (17). These results confirmed that eIF2B function is impaired in yeast cells when eIF2 is hyperphosphorylated on Ser-51, and they lent further support to the idea that GCN3 makes eIF2B more sensitive to inhibition by eIF2(αP).

Biochemical studies with mammalian systems have shown that eIF2(αP) · GDP is an inhibitor that binds to eIF2B and interferes with the recycling of nonphosphorylated eIF2. This

* Corresponding author. Mailing address: Laboratory of Eukaryotic Gene Regulation, National Institute of Child Health and Human Development, Building 6B, Room 3B-309, 6 Center Dr., Bethesda, MD 20892-2785. Phone: (301) 496-4480. Fax: (301) 496-0243. E-mail: ahinnebusch@nih.gov.

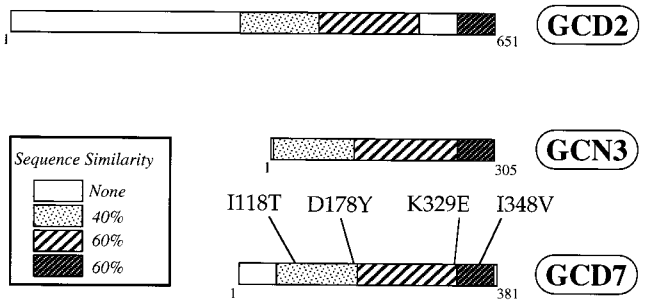

FIG. 1. Regions of sequence homology between the GCD2, GCD7, and GCN3 subunits of eIF2B in yeast. The protein-coding sequences of GCD2, GCD7, and GCN3 are depicted schematically from the N terminus to the C terminus (left to right, with the terminal amino acids numbered) as open bars with shaded segments indicating regions of sequence similarity shared by all three proteins. The positions of missense substitutions isolated previously (47) in GCD7 that confer resistance to the growth-inhibitory effects of eIF2(αP) in vivo are shown above the sequence. In GCD2, the two regions with 60% sequence similarity to GCD7 and GCN3 are interrupted by a region that shows no sequence homology with GCD7 or GCN3.

causes complete inhibition of protein synthesis even when only a fraction of eIF2 is phosphorylated. One proposed mechanism suggests that dissociation of the eIF2B · eIF2(αP) · GDP complex is extremely slow, such that eIF2B is, in effect, bound irreversibly by phosphorylated eIF2. Because eIF2 is in a considerable excess with respect to eIF2B, phosphorylation of only a small fraction of eIF2 would be sufficient to sequester all of the eIF2B in inactive complexes. An alternative model suggests that eIF2(αP) has a much greater rate of association with eIF2B than does nonphosphorylated eIF2, allowing eIF2(αP) to act as a competitive inhibitor without forming an excessively stable eIF2B · eIF2(αP) · GDP complex. The latter hypothesis is consistent with biochemical studies by Rowlands et al. (39), using highly purified mammalian eIF2 and eIF2B, and with the in vivo effects of overproducing eIF2 in yeast cells containing an activated eIF2α kinase (17). However, little is known at the molecular level about how eIF2 phosphorylation affects its affinity for eIF2B or inhibits nucleotide exchange.

eIF2B is atypical of guanine nucleotide exchange factors in containing so many subunits. For example, the exchange factor for RAS in *Saccharomyces* is the single polypeptide encoded by *CDC25* (4). The subunit complexity of eIF2B could reflect its regulation by phosphorylated eIF2, and the fact that GCN3 is required primarily for inhibition by eIF2(αP) is in accord with this idea. Genetic evidence suggests that GCD7 and GCD2 also have roles in this regulatory mechanism. First, GCN3, GCD7, and the C-terminal half of GCD2 have sequence similarity with each other (Fig. 1) (5). Also, four point mutations in *GCD7* and a single mutation in *GCD2* were isolated in a random screen for mutations that mimic deletion of *GCN3* by reversing the toxicity of eIF2 hyperphosphorylation on cell growth (Fig. 1) (47). As expected, many *GCN3* mutations were also obtained in this screen; however, no mutations in *GCD1* or *GCD6* were isolated. These results led to the idea that GCD2, GCD7, and GCN3 have important functions in the regulation of eIF2B activity, whereas GCD1 and GCD6 could be involved principally in catalysis (22). We recently obtained biochemical evidence to support this view by showing that overexpression of GCD2, GCD7, and GCN3 leads to the formation of a stable subcomplex containing only these three subunits of eIF2B. Overexpression of this trimeric subcomplex partially suppressed the toxicity of eIF2 phosphorylation without increasing the catalytic activity of eIF2B, presumably by sequestering eIF2(αP) and allowing native eIF2B to exchange the nonphosphorylated eIF2 (52). These results support the idea that GCD2, GCD7, and GCN3 form a regulatory domain in eIF2B that interacts with eIF2(αP).

To test our hypothesis that GCD2 plays an important role in the regulation of eIF2B by eIF2(αP) and to identify residues in GCD2 critical for this function, we set out to isolate *GCD2* mutations that render eIF2B insensitive to eIF2(αP) without reducing the catalytic activity of the recycling factor. We isolated nine regulatory mutations that, in agreement with our model, alter residues only in the C-terminal half of GCD2, which has sequence similarity with GCD7 and GCN3. Interestingly, the *GCD2* mutations and additional regulatory mutations that we isolated subsequently in *GCD7* and *GCN3* cluster in two segments of ca. 70 residues in length, both of which are within the region of sequence similarity. Moreover, in several instances we recovered mutations that alter homologous positions in two or all three of the subunits. These results imply that structurally related segments in GCD2, GCD7, and GCN3 are devoted to the regulatory interactions between eIF2B and eIF2. We propose that these three subunits employ homologous structural elements to form a single regulatory domain on eIF2B, in which each subunit makes independent contacts with eIF2α at points surrounding the phosphorylation site at Ser-51. This structural organization would enable eIF2B to assess the phosphorylation state of bound eIF2. The mutations described here would disrupt one of these interactions with eIF2α or alter the interplay between eIF2B subunits, so that eIF2B fails to discriminate between eIF2 and eIF2(αP) and allows nucleotide exchange on the phosphorylated substrate.

MATERIALS AND METHODS

Plasmids. The following plasmids were constructed previously: (i) derivatives of the single-copy *CEN4 URA3* plasmid YCp50 (37) bearing *GCN3* (Ep69) (19) or *gcn2-507* (p591) (50); (ii) derivatives of the low-copy-number *CEN6 URA3* plasmid pRS316 (42) that contain *GCN2* (p722), *GCN2^c-513* (*GCN2^c-M719V,E1537G*) (p1052), *GCN2^c-516* (*GCN2^c-E532K,E1522K*) (p1056), no insert (p713) (35), *SUI2* (encoding eIF2α) (p919) (16), or *GCD7* (pJB99) (5); (iii) high-copy-number 2μm *URA3* plasmids with a *GAL-CYC* promoter driving expression of the cDNAs encoding wild-type PKR (p1420) or the catalytically defective mutant PKR-K296R (p1421) (15); (iv) the high-copy-number 2μm *URA3 GCD2* plasmid pCP57 (6); (v) derivatives of the low-copy-number *CEN6 LEU2* plasmid pRS315 (42) containing *GCD7* (p1305 and p1558), *GCD7-1118T* (p1559), *GCD7-D178Y* (p1560), *GCD7-K329E* (p1561), *GCD7-1348V* (p1562), or *GCD7-1118T,D178Y* (p1563) (47); (vi) the low-copy-number *LEU2 CEN4*, plasmids bearing *SUI2* (p1097), *SUI2-S51A* (p1098), *SUI2-S51D* (p1101) (16), and *SUI2-L84F* (p1350) (46); (vii) the high-copy-number 2μm *TRP1* plasmids derived from pRS424 (9) containing the *GAL-CYC* promoter fused to the cDNAs encoding wild-type PKR (p1545) or the PKR-K296R mutant (p1548) (35a); and (viii) the high-copy-number *URA3 GCN3* plasmid p2304 (52).

The following plasmids were constructed in this study by standard methods (40). pCP62 contains *GCD2* on a 2.6-kb *Sal*I-*Eag*I fragment subcloned from pCP46 (33) into similarly cut YCp50 (32a). The *gcd2Δ::hisG* plasmid pAV1001 was generated by removing the region between the *Bgl*II site 5′ of the coding region of *GCD2* and the *Eco*RI site near the C terminus in plasmid pCP46 and replacing it with the *hisG-URA3-hisG* cassette isolated on a *Bgl*II-*Bam*HI fragment from pNKY51 (1). The *Eco*RI and *Bam*HI ends were end filled with Klenow polymerase prior to ligation. The *GCD2 LEU2 CEN4* plasmid pAV1002 was constructed by ligating the *GCD2 Xho*I-to-*Xba*I fragment isolated from pCP46 with *Bam*HI-cut pSB32 (38) after end filling of both fragments with Klenow polymerase. pAV1003 is a *GCD2 CEN4 TRP1* plasmid made by removing the *URA3* gene from pCP62 by digestion with *Eag*I and *Spe*I and ligating the plasmid to the *TRP1* gene from pRS304 isolated on an *Ssp*I fragment (42) after end filling both fragments with Klenow polymerase. pAV1026 was derived from plasmid pAV1003 in two steps: (i) a region of the *tet* gene was removed by *Cla*I digestion and religation, generating pAV1014, and (ii) site-directed mutagenesis was used, as described below, to make a silent mutation in *TRP1* that eliminated the *Ban*II site. As a result, the *Nsi*I, *Nru*I, *Bam*HI, *Ban*II, and *Cla*I sites in *GCD2* are unique in pAV1026. p2297 is a high-copy number *URA3 GCD2* plasmid constructed by deletion of *GCD7* and *GCN3* from p1871 (17) by *Not*I digestion and religation.

Isolation of regulatory mutations in *GCD2*, *GCD7*, and *GCN3*. Three different random mutagenesis procedures were employed to isolate a pool of mutated plasmid DNA from which mutations with the desired phenotype were selected. UV mutagenesis was used for generating *GCD2* mutations. While this was

successful, other, more rapid, random mutagenesis procedures became available, so these were employed instead to generate *GCD7* and *GCN3* mutations. In addition, it was necessary to isolate dominant mutations in *GCN3*, as it is nonessential and recessive loss-of-function alleles would also satisfy the selection procedure. This was accomplished by mutagenizing the gene on a high-copy-number plasmid and screening the mutant plasmids for the desired phenotype in a wild-type *GCN3* strain. The same strategy was used to isolate dominant *GCD2* alleles in an effort to identify mutations that alter GCD2 function without diminishing its capacity for complex formation with other subunits. When the *GCD2* alleles thus obtained were analyzed on low-copy-number vectors, their dominance over wild-type *GCD2* was diminished. *GCD7* was mutagenized on a single-copy plasmid, and plasmid shuffling (3) was used to identify mutant alleles as the only resident copy of *GCD7*. *GCD7* alleles with the strongest phenotypes were found to be semidominant over wild-type *GCD7*.

***GCD2* mutagenesis.** Plasmid pCP57 (6), a high-copy-number *URA3* plasmid containing the entire *GCD2* gene, was subjected to UV mutagenesis in vitro as described previously (35). Following irradiation, plasmid DNA from ca. 4,000 pooled bacterial transformants was introduced (25) into yeast strain H1613 containing *GCD2* and the *GCN2^c-516* allele, which confers a Slg$^-$ phenotype (see the introduction). Fast-growing transformants containing plasmid-borne regulatory mutations were identified on the basis of reversion to the Slg$^-$ phenotype when the plasmid was evicted by growth on medium containing 5-fluoroorotic acid (5-FOA) (3). Plasmid DNAs from 63 plasmid-dependent revertants of H1613 were pooled and subcloned into the *TRP1 GCD2* plasmid pAV1026 to create four pools of plasmids, each containing a different region of mutagenized *GCD2*. Each plasmid pool was introduced into the *gcd2Δ::hisG GCN2 his1-29* strain GP3173 by plasmid shuffling. Three hundred Ura$^-$ Trp$^+$ transformants from each pool were screened for sensitivity to 3-aminotriazole (3AT), an inhibitor of histidine biosynthesis, as described previously (24). 3AT-sensitive transformants were obtained only from pools constructed from fragments encoding the C-terminal half of *GCD2*; 80 of these transformants were from plasmids bearing the 560-bp *Bam*HI-*Ban*II fragment, and 171 were from plasmids containing the 757-bp *Ban*II-*Cla*I fragment. No 3AT-sensitive transformants were isolated from the pools containing the 815-bp *Nsi*I-*Nru*I or 457-bp *Nru*I-*Bam*HI mutagenized fragments encoding the N-terminal half of GCD2. DNA sequence analysis of the subcloned *GCD2* fragments in a representative sample of plasmids isolated from the 3AT-sensitive transformants identified seven independent single mutations and one double mutation of adjacent residues in *GCD2*. The following plasmids contain these eight alleles: pAV1030 (*GCD2-E377K*) and pAV1031 (*GCD2-L381Q*), derived from the *Bam*HI-*Ban*II subcloned mutant DNA pool; and pAV1032 (*GCD2-F523I*), pAV1033 (*GCD2-K627T*), pAV1034 (*GCD2-T630S*), pAV1035 (*GCD2-A634D*), pAV1036 (*GCD2-P636T*,*P637L*), and pAV1037 (*GCD2-P641F*), derived from the *Ban*II-*Cla*I subcloned mutant pool.

GCD2-I625F was isolated in a separate screen by using error-prone PCR as described previously (7). The 349-bp *GCD2* fragment from position +1554 to +1902 relative to the AUG start codon was amplified from plasmid p2297, digested with *Nhe*I and *Eco*RI, and used to replace the corresponding wild-type fragment in p2297. The resulting pool of plasmids was screened for reversion of the Slg$^-$ phenotype of strain H1613 as described above. The PCR-mutagenized fragment in each plasmid bearing a *GCD2* suppressor was sequenced in its entirety, identifying two alleles containing single-amino-acid substitutions: *GCD2-I625F* (borne on plasmid pWM71) and *GCD2-K627T*. The latter was also isolated in the screen of UV-mutagenized *GCD2* DNA and was not characterized further. pAV1107 (*GCD2-I625F*) was generated by replacing the *GCD2* *Bam*HI-*Cla*I fragment in pAV1026 with the corresponding fragment from pWM71.

***GCD7* mutagenesis.** The bacterial mutator strain XL1-Red (Stratagene, La Jolla, Calif.) was used according to the manufacturer's instructions to mutate 0.3 μg of the low-copy-number *GCD7 LEU2* plasmid p1305 (47). Plasmid DNA from a pool of 15,000 transformants was introduced into the *gcd7Δ* strain H2217 containing wild-type *GCD7* on pJB99. The transformants were pooled, and plasmid shuffling was used to evict pJB99. The resulting Ura$^-$ strains (ca. 30,000) were transformed with the *URA3 GCN2^c-516* plasmid p1056. From ca. 20,000 of these transformants, 764 fast-growing revertants were selected. Plasmid p1056 was evicted from the revertants on 5-FOA medium, and the Ura$^-$ strains thus obtained were screened for 3AT sensitivity. Fifty-two mutants showed increased sensitivity to 3AT over that of the wild-type *GCD7* strain. Of these, 47 yielded plasmids that conferred the 3AT-sensitive phenotype upon reintroduction into strain H2217. Complete nucleotide sequencing of *GCD7* in each plasmid identified 11 novel single mutations, which were subcloned into the unmutagenized low-copy-number *GCD7 LEU2* plasmid p1558 (47), as follows: pAV1077 (*GCD7-F82L*), pAV1078 (*GCD7-L117S*), and pAV1079 (*GCD7-S119P*) contain subcloned *Xba*I-*Sac*I fragments; pAV1081 (*GCD7-G218R*) and pAV1082 (*GCD7-R254C*) contain subcloned *Sac*I-*Ava*I fragments; and pAV1083 (*GCD7-P291S*), pAV1084 (*GCD7-V292A*), pAV1085 (*GCD7-Y305C*), pAV1086 (*GCD7-P306L*), pAV1087 (*GCD7-N357I*), and pAV1088 (*GCD7-S359G*) contain subcloned *Ava*I-*Eag*I fragments. These plasmids were resequenced to confirm the presence of each mutation.

***GCN3* mutagenesis.** Random mutagenesis of *GCN3* was performed by using PCR as previously described (7). Plasmids containing *GCN3* alleles with mutations in the N-terminal portion of the coding region were constructed by amplifying the 843-bp *Hin*dIII-*Cla*I fragment of *GCN3* with oligonucleotide primers GN31 (5′ GAT ACG ACA CAG CAA CAT TGT CGC C) and GN32 (5′ CCA ACG AAC ACT TTG TCA ACC TAT TCG) and inserting the mutagenized fragments between the corresponding sites of the 2μm *URA3 GCN3* plasmid p2304. Plasmid DNA was pooled from ca. 20,000 bacterial transformants. Similarly, *GCN3* alleles with mutations in the C-terminal portion of the coding region were constructed by using oligonucleotides GN33 (5′ CGA TAG CGC GGT TGG GCG GTA ATCG) and GN34 (5′ GGG GGG ATC CAG TTT CAC ATA AAG GAT GCT CTC TTG CGC) as PCR primers to amplify the 466-bp *Cla*I-*Bam*HI *GCN3* fragment that was used to replace the corresponding fragment in p2304. Mutagenized plasmid DNA was prepared from a pool of 150,000 bacterial transformants.

Dominant Gcn$^-$ alleles of *GCN3* were selected as described above for the *GCD2* regulatory alleles by transforming strain H1613 with the two pools of mutagenized *GCN3* plasmids and selecting the fastest-growing revertants. For the N-terminal library, 58 plasmid-dependent revertants were isolated from ca. 10,000 yeast transformants. Sequence analysis of the mutagenized fragments in nine plasmids identified the following five plasmids containing *GCN3* alleles with single amino acid substitutions: pWY03 (*GCN3-T41A*), pWY06 (*GCN3-E44V*), pWY07 (*GCN3-N80D*), pWY11 (*GCN3-F73L*), and pWY12 (*GCN3-E44K*). From the C-terminal library, 22 revertants were isolated from 54,000 yeast transformants, and sequence analysis of the mutagenized fragments identified four plasmids containing *GCN3* alleles with single amino acid changes: pWY101 (*GCN3-T291P*), pWY103 (*GCN3-F240I*), pWY106 (*GCN3-F240L*), and pWY115 (*GCN3-S293R*).

Site-directed mutagenesis. Site-directed mutagenesis was performed with the Altered Sites II mutagenesis kit (Promega Corp., Madison, Wis.) by using the protocol provided and synthetic oligonucleotides containing the desired nucleotide changes. A derivative of pAlter-1 (Promega Corp.) containing a 3.65-kb *Hin*dIII fragment from pAV1014 containing *GCD2* and *TRP1* (pAV1018) was employed. The *Ban*II site in *TRP1* was eliminated in pAV1018 by silent mutagenesis with the oligonucleotide GDP115 (5′ ACT GGG TTG GAA GGC AAG AAA GTC CCG AAA GCT TGA GTA TTC). Mutagenesis was verified by restriction digestion. The mutagenized *Hin*dIII fragment was subcloned back into pAV1014 to generate pAV1026. Specific codons of *GCD2* were altered as follows: *gcd2-P502S* with primer GDP149 (5′ TCG CAG CAG ACA ATT ACA GAA ATA TTT CTT CTC TTA GCGC), incorporating a novel *Ssp*I site; *gcd2-S638R* with primer GDP150 (5′ TAA AAT AAC AGG GAC AGA TCT AGG TGG CAA AGC GCC GAAT), incorporating a novel *Bgl*II site; and *gcd2-S638C* with primer GDP152 (5′ TCT TAA AAT AAC AGG GAC ACT GCA GGG TGG CAA AGC GCC GAA TT), incorporating a novel *Pst*I site. Mutagenesis was verified by restriction digestion and DNA sequence analysis of the *GCD2* DNA within the *Hin*dIII fragment, after which the appropriate *Hin*dIII fragment was subcloned into pAV1026, generating the following plasmids: pAV1102 (*gcd2-P502S*), pAV1104 (*gcd2-S638R*), and pAV1105 (*gcd2-S638C*).

Genetic methods and yeast strain constructions. Standard methods were used for culturing, transformation, and construction of yeast strains (25, 41). Tests for sensitivity to amino acid analogs have been described previously (24). Table 1 shows the yeast strains used in this study. All are derived from strain S288C. For the studies comparing plasmid-borne mutations in *GCD2*, *GCD7*, or *GCN3* (results shown in Fig. 2 to 4, 6, and 7), only the recipient yeast strains (GP3040, GP3140, GP3160, GP3224, GP3514, H1607, H1613, H2218, H2220, and Y117) are listed in Table 1. Recipient strains bearing chromosomal deletions of *GCD2* or *GCD7* carried a plasmid-borne wild-type allele of the corresponding gene on a *URA3* plasmid (pCP62 for *GCD2* and pJB99 for *GCD7*) that was evicted by growth on 5-FOA medium following introduction of the mutant alleles. Deletion of *GCN2* in strains H1515, GP3040, H1645, and GP3153 to generate strains GP3140, GP3224, GP3514, and Y117, respectively, was carried out by using plasmid p1144 as described previously (16). Disruption of *GCN3* with the *LEU2* gene in strains H1515 and GP3040 to generate strains GP3153 and GP3160, respectively, was conducted with plasmid Ep146 as described previously (19). Deletion of *GCD2* in strains H1515 and H1645 to generate strains GP3040 and GP3514, respectively, was performed as follows. (i) Plasmid shuffling on 5-FOA medium was used to exchange p919 (*SUI2 URA3*) with p1097 (*SUI2 LEU2*) in H1645. (ii) Plasmids containing *GCD2*, i.e., pAV1002 (*GCD2 LEU2*) for H1515 and pAV1003 (*GCD2 TRP1*) for H1645, were introduced, and the chromosomal copy of *GCD2* was deleted by transforming with plasmid pAV1001, bearing the *gcd2Δ::hisG-URA3-hisG* allele, after digestion with *Xba*I and *Sal*I. The *hisG-URA3-hisG* cassette was evicted by growth on 5-FOA medium, leaving the *gcd2Δ::hisG* allele in the chromosome (1). (iii) Southern hybridization analysis (43) was carried out to confirm the replacement of chromosomal *GCD2* with the *gcd2Δ::hisG* allele by digesting chromosomal DNA with *Xba*I and *Hpa*I and using the 1,470-bp *Stu*I-*Xba*I *GCD2-hisG* fragment from pAV1001 as the hybridization probe (data not shown). Strain GP3173 is a meiotic segregant of a cross between GP3040 and H1486.

Isoelectric-focusing gel electrophoresis and detection of eIF2α phosphorylation. One-dimensional isoelectric-focusing polyacrylamide gel electrophoresis was carried out on total cellular proteins, followed by immunoblot analysis with antibodies against eIF2α and detection of immune complexes with enhanced chemiluminescence (Amersham) exactly as described previously (16) except for the addition of 2-aminopurine to the cell-breaking buffer (36). The percentage of

TABLE 1. Yeast strains

Strain[a]	Genotype	Construction	Source or reference
GP3040	*MAT***a** *leu2-3 leu2-112 ura3-52 trp1-Δ63 gcd2Δ::hisG* pCP62 (*GCD2 URA3*)	*gcd2*Δ in H1515	This study
GP3140	*MAT***a** *leu2-3 leu2-112 ura3-52 trp1-Δ63 gcn2*Δ	*gcn2*Δ in H1515	This study
GP3153	*MAT***a** *leu2-3 leu2-112 ura3-52 trp1-Δ63 gcn3Δ::LEU2*	*gcn3Δ::LEU2* in H1515	This study
GP3160	*MAT***a** *leu2-3 leu2-112 ura3-52 trp1-Δ63 gcd2Δ::hisG gcn3Δ::LEU2* pCP62 (*GCD2 URA3*)	*gcn3Δ::LEU2* in GP3040	This study
GP3173	*MAT***a** *his1-29 leu2-3 leu2-112 ura3-52 trp1-Δ63 gcd2Δ::hisG* pCP62 (*GCD2 URA3*)	Meiotic segregant of GP3040 × H1486	This study
GP3224	*MAT***a** *leu2-3 leu2-112 ura3-52 trp1-Δ63 gcn2*Δ *gcd2Δ::hisG* pCP62 (*GCD2 URA3*)	*gcn2*Δ in GP3040	This study
GP3514	*MAT***a** *leu2-3 leu2-112 ura3-52 trp1-Δ63 gcn2*Δ *gcd2Δ::hisG sui2*Δ[b] p919 (*SUI2*[b] *URA3*) pAV1003 (*GCD2 TRP1*)	*gcd2*Δ then *gcn2*Δ in H1645	This study
H1486	*MAT*α *his-1-29 leu2-3 leu2-112 ura3-52 HIS4-lacZ*		49
H1515	*MAT***a** *leu2-3 leu2-112 ura3-52 trp1-Δ63*		16
H1607	*MAT*α *ino1 leu2-3 leu2-112 ura3-52 GCN2*[c]*-513 HIS4-lacZ*		35
H1613	*MAT*α *ino1 leu2-3 leu2-112 ura3-52 GCN2*[c]*-516 HIS4-lacZ*		35
H1645	*MAT***a** *leu2-3 leu2-112 ura3-52 trp1-Δ63 sui2*Δ p919 (SUI2 URA3)		16
H2217	*MAT***a** *leu2-3 leu2-112 ura3-52 trp1-Δ63 gcd7Δ::hisG (GCN4-lacZ TRP1)* pJB99 (*GCD7 URA3*)		47
H2218	*MAT***a** *leu2-3 leu2-112 ura3-52 trp1-Δ63 gcn2*Δ *gcd7Δ::hisG* (*GCN4-lacZ TRP1*) pJB99 (*GCD7 URA3*)		47
H2220	*MAT***a** *leu2-3 leu2-112 ura3-52 trp1-Δ63 gcn3*Δ *gcd7Δ::hisG* (*GCN4-lacZ TRP1*) pJB99 (*GCD7 URA3*)		47
Y117	*MAT***a** *leu2-3 leu2-112 ura3-52 trp1-Δ63 gcn3Δ::LEU2 gcn2*Δ	*gcn2*Δ in GP3153	This study

[a] All strains except strains GP3173, H1486, H1607, and H1613 are isogenic to strain H1515. Strains H1607 and H1613 are isogenic to each other.
[b] *SUI2* is the yeast gene encoding eIF2α.

eIF2α that was phosphorylated at Ser-51 was determined by densitometry of autoradiograms.

Multiple sequence alignment. The following sequences were obtained from the GenBank sequence database (with accession numbers shown in parentheses): GCN3 (P14741), GCD2 (P12754), GCD7 (P32502), *Caenorhabditis elegans* eIF2Bα (P34604), rat eIF2Bα (U05821), and rat eIF2Bδ (Z48225). The human eIF2Bβ sequence (L4039) obtained from a full-length cDNA clone was identified in a BLAST search (2) and modified after alignment with 16 short overlapping sequences covering the entire sequence from the expressed sequence tag database (dbEST). Modifications included resolution of ambiguous nucleotides and minor reading frame adjustments to generate a full-length sequence that was nearly identical to the recently published rabbit sequence (13). The multiple sequence alignment shown in Fig. 5B and C was created with the program PileUp and reformatted with the programs LineUp and Pretty (Wisconsin Sequence Analysis Package version 8.1; Genetics Computer Group, Madison, Wis.). Highlighting of sequence homologies was done manually with the drawing program Canvas version 3.04 (Deneba Software, Miami, Fla.).

Coimmunoprecipitation of eIF2B subunits. Ribosomal salt wash (RSW) fractions were prepared from 1 liter of yeast cells grown in yeast extract-peptone-dextrose medium to an optical density at 600 nm of approximately 6, as described previously (17). Coimmunoprecipitation of eIF2B subunits with anti-GCD6 antiserum was performed as described previously (6, 17) except that 4 μl of GCD6-specific antiserum or 10 μl of preimmune antiserum was used to immunoprecipitate eIF2B from 400 μg of RSW.

RESULTS

Regulatory mutations in the GCD2 subunit of eIF2B cluster within regions of sequence similarity between GCD2, GCD7, and GCN3. Previously, we hypothesized that regions of GCD2 and GCD7 that have sequence homology with GCN3 would be important for negative regulation of eIF2B by eIF2(αP) (22). The fact that only the C-terminal half of GCD2 has sequence similarity with GCD7 and GCN3 allowed us to test this idea. We reasoned that it should be possible to isolate single amino acid substitutions in GCD2 which render eIF2B insensitive to eIF(2αP) and that many of these mutations would be restricted to regions of sequence similarity between GCD2, GCD7, and GCN3. To isolate *GCD2* regulatory mutations, we performed in vitro mutagenesis of the entire cloned gene and screened mutagenized plasmids for suppression of the slow-growth phenotype (Slg^-) due to eIF2α hyperphosphorylation by an activated GCN2 kinase. High-copy-number *GCD2* plasmid DNA was mutagenized by UV irradiation and introduced into a *GCD2 GCN2*[c]*-516* yeast strain (H1613), after which dominant *GCD2* mutations were selected as fast-growing (Slg^+) revertants (see Materials and Methods). By this approach, we identified eight independent suppressor alleles, seven containing single missense mutations and one with a pair of mutations at adjacent residues in the *GCD2* coding sequence (*P636T* and *P637L*) (Fig. 2A). One additional allele was generated by PCR amplification of *GCD2* and identified by the same screening procedure. Interestingly, all of the substitutions were located in regions of sequence similarity between GCD2, GCD7, and GCN3 in the C-terminal half of GCD2. In addition, the mutations appeared to cluster at three sites in this portion of *GCD2*, with the majority mapping in the most highly conserved segment near the C terminus. The suppressor phenotype of these alleles was evident in the presence of chromosomally encoded *GCD2*, suggesting that the mutant proteins compete with wild-type GCD2 for incorporation into eIF2B and decrease the sensitivity of the mutant complex to eIF2(αP).

To characterize the effects of these suppressor mutations when the mutant proteins were expressed as the only GCD2 present in the cell, we subcloned all nine mutant alleles onto single-copy plasmids and introduced them by plasmid shuffling (3) into yeast strains with the chromosomal *GCD2* gene deleted. In these strains all of the suppressor alleles fully reverted the Slg^- phenotype of *GCN2*[c]*-516*, the allele which they were selected to suppress (Fig. 2B). We also examined whether the *GCD2* alleles would interfere with the ability of wild-type GCN2 to stimulate translation of *GCN4* mRNA in response to amino acid starvation. As described in the introduction, the level of *GCN4* translation is very sensitive to reductions in the activity of eIF2B. A simple and well-characterized assay for *GCN4* translation is to monitor growth of yeast in the presence of 3AT, an inhibitor of the *HIS3*-encoded step in histidine biosynthesis. Histidine deprivation causes an accumulation of uncharged $tRNA^{His}$, which stimulates the ability of GCN2 to phosphorylate eIF2 and thereby inhibit eIF2B. The resulting reduction in ternary complex levels causes increased GCN4

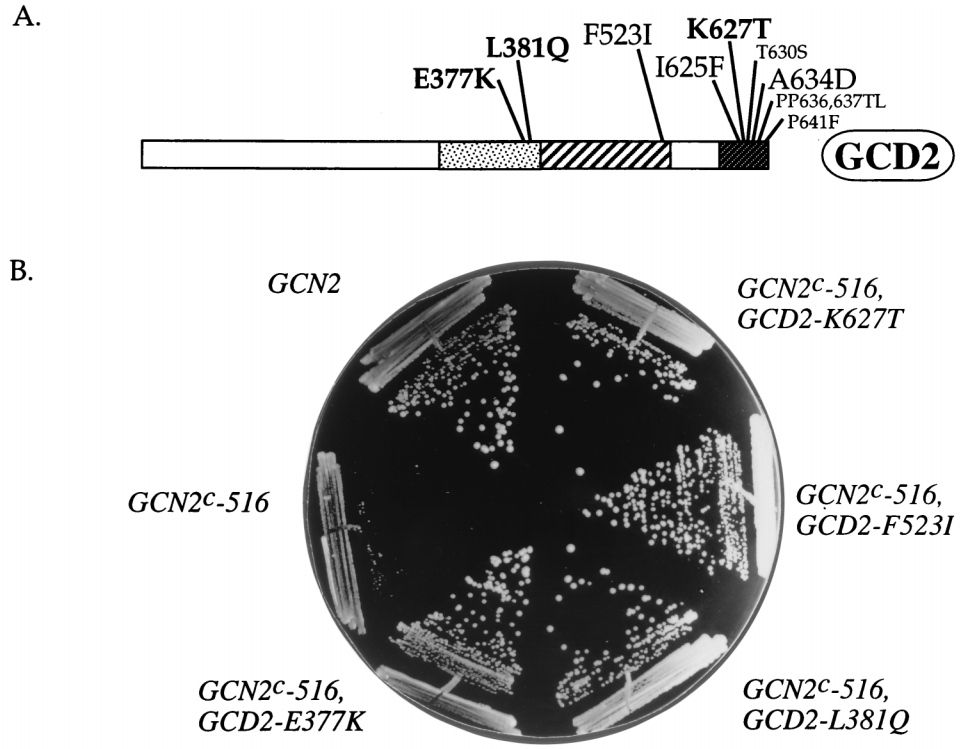

C.

GCD2 Allele	Relevant genotype: *gcd2Δ, gcn2Δ*				
	GCN2		*GCN2c-513*		PKR
	SD	3AT	SD	3AT	SGAL
GCD2	5+	3+	1+	2+	0
E377K	5+	0	5+	1+	3+
L381Q	5+	0	5+	0	4.5+
F523I	5+	2+	2+	3+	1+
I625F	5+	2+	2+	3+	1+
K627T	5+	0	5+	0	4.5+
T630S	5+	2+	2+	3+	+/-
A634D	5+	1+	3+	3+	1.5+
P636T,P637L	5+	2+	2+	3+	+/-
P641F	5+	2+	2+	3+	-/+

FIG. 2. Genetic analysis of regulatory mutations in *GCD2*. (A) Locations of *GCD2* regulatory mutations. The GCD2 protein sequence is depicted as in Fig. 1, showing the locations of the regulatory mutations isolated in this study. The font size is proportional to the degree to which regulation of translation by phosphorylated eIF2 is impaired by the mutation, based on the results shown in panel C. (B) *GCD2* regulatory mutations suppress the Slg$^-$ phenotype of a hyperactive GCN2^c kinase. Transformants of *gcd2Δ gcn2Δ* strain GP3224 bearing the wild-type or the indicated mutant allele of *GCD2* and the indicated allele of *GCN2* were streaked for single colonies on minimal medium (SD) supplemented with leucine, isoleucine, and valine and grown for 2.5 days at 30°C. (C) Summary of genetic analysis. The growth of transformants of *gcd2Δ gcn2Δ* strain GP3224 bearing one plasmid containing the indicated *GCD2* allele (see Materials and Methods for plasmid designations) and a second plasmid containing either wild-type *GCN2* (p722), the *GCN2^c-513* allele (p1052), or PKR cDNA under the control of a hybrid *GAL10-CYC1* promoter (p1420) was examined as follows: (i) by streaking for single colonies on SD minimal medium, with the maximum growth rate designated 5+; (ii) by replica plating on SD medium supplemented with 3AT to induce histidine starvation, with the maximum growth rate designated 3+; and (iii) by streaking for single colonies on minimal medium containing galactose in place of glucose as a carbon source (SGAL), with the maximum growth rate designated 5+. In each case, no detectable growth was scored as 0, and 1+ > +/− > −/+ > 0. Mutations that rendered strains completely or largely insensitive to the effects of eIF2 phosphorylation are shaded.

synthesis and *HIS3* transcription. Thus, regulatory mutations in eIF2B that prevent increased *GCN4* translation in response to histidine starvation decrease the ability of these cells to grow in the presence of 3AT. All nine *GCD2* suppressors conferred increased sensitivity to 3AT in strains bearing wild-type *GCN2*. Three of the *GCD2* suppressors (*GCD2-E377K*, *-L381Q*, and *-K627T*) showed the same 3AT sensitivity conferred by deletion of *GCN2*, suggesting that little or no increase in *GCN4* expression occurred in response to eIF2 phosphorylation in these mutants (Gcn$^-$ phenotype). The other six *GCD2* mutations appeared to reduce, but not abolish, derepression of *GCN4* and *HIS3* expression in response to eIF2(αP), as they showed only decreased resistance to 3AT (Fig. 2C).

Resistance to 3AT in strains with *GCN2* deleted is a very sensitive indicator of reduced catalytic function of eIF2B and has been used to isolate many reduced-function mutations in eIF2B subunits (10, 20). To assess whether any of the regulatory mutants isolated here also showed a catalytic defect, the growth of *gcn2Δ* strains bearing the *GCD2* suppressor alleles on medium containing 3AT was examined. None of the *GCD2* suppressors described here (or the *GCD7* and *GCN3* suppressors described below) led to detectable growth on 3AT medium in the *gcn2Δ* background (data not shown). In addition, none of the suppressors reduced the rate of colony formation in the *GCN2* strains under nonstarvation conditions (Fig. 2C, SD medium). Together these results indicate that the suppressor mutations do not impair the catalytic activity of eIF2B.

We also tested the *GCD2* suppressors in a strain bearing *GCN2^c-513*, encoding a hyperactivated kinase that phosphorylates eIF2 in vivo at higher levels than are produced by the *GCN2^c-516* allele used in the genetic selection (35). The three *GCD2* alleles with the strongest Gcn$^-$ phenotype in the *GCN2* strain were also completely sensitive to 3AT and fully suppressed the Slg$^-$ phenotype on SD medium in the *GCN2^c-513* background. Similarly, the *GCD2* alleles with a weaker Gcn$^-$

A.

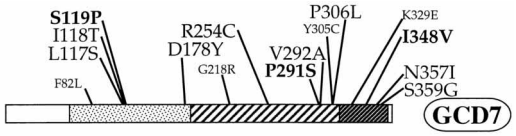

B.

GCD7 Allele	Relevant genotype				
	gcd7Δ, gcn2Δ				
	GCN2		*GCN2^c-513*		PKR
	SD	3AT	SD	3AT	SGAL
GCD7	5+	3+	1+	1.5+	0
F82L	5+	1+	4+	2+	+/-
L117S	5+	1+	4.5+	2+	1+
I118T	5+	+/-	5+	2+	2+
S119P	5+	0	5+	0	4.5+
D178Y	5+	2+	5+	3+	1+
I118T, D178Y	5+	0	5+	0	4.5+
G218R	5+	3+	3+	3+	+/-
R254C	5+	0	5+	1+	2+
P291S	5+	0	5+	1+	3+
V292A	5+	3+	4+	3+	1+
Y305C	5+	3+	4+	3+	+/-
P306L	5+	1+	4+	3+	1+
K329E	5+	3+	3+	3+	-/+
I348V	5+	0	5+	1+	3+
N357I	5+	1+	5+	3+	1+
S359G	5+	+/-	5+	3+	2+

FIG. 3. Genetic analysis of regulatory mutations in *GCD7*. (A) Locations of *GCD7* regulatory mutations. The GCD7 protein sequence is depicted as in Fig. 1, showing the locations of the regulatory mutations isolated in this study together with the four mutations characterized previously (47). The font size is proportional to the degree to which regulation of translation by phosphorylated eIF2 is impaired by the mutation, based on the results shown in panel B. (B) Summary of genetic analysis. Transformants of *gcd7Δ gcn2Δ* strain H2218 bearing one plasmid containing the indicated *GCD7* allele (see Materials and Methods for plasmid designations) and a second plasmid containing either wild-type *GCN2*, *GCN2^c-513*, or the PKR cDNA under the control of a hybrid *GAL10-CYC1* promoter were obtained. Growth was examined as described in the legend to Fig. 2C. *GCD7* mutations that rendered strains completely or largely insensitive to the effects of eIF2 phosphorylation are shaded.

A.

B.

GCN3 Allele	Relevant genotype			
	GCN2^c -513		*gcn2Δ*	*gcn2Δ, gcn3Δ*
			+ PKR	+ PKR
	SD	3AT	SGAL	SGAL
Vector	1+	2+	0	2+
GCN3	1+	2+	0	0
T41A	5+	0	4+	4.5+
E44K	5+	0	4+	4.5+
E44V	5+	0	4+	4.5+
F73L	5+	0	4+	4.5+
N80D	5+	0	4+	4.5+
F240I	5+	0	4+	4.5+
F240L	5+	0	4+	4.5+
T291P	5+	0	4+	4.5+
S293R	5+	0	4+	4.5+

FIG. 4. Genetic analysis of regulatory mutations in *GCN3*. (A) Locations of *GCN3* regulatory mutations. The GCN3 protein sequence is depicted as in Fig. 1, showing the locations of the regulatory mutations isolated in this study. (B) Summary of genetic analysis. The indicated *GCN3* allele (see Materials and Methods for plasmid designations) on a high-copy-number *URA3* plasmid was introduced into strains H1613 (*GCN2^c-516*) and H1607 (*GCN2^c-513*) or introduced together with a second plasmid expressing the PKR cDNA from a hybrid *GAL10-CYC1* promoter (p1545) into strains GP3140 (*gcn2Δ*) and Y117 (*gcn2Δ gcn3::LEU2*). The growth of these transformants was examined as described in the legend to Fig. 2C. All of the *GCN3* mutations rendered the strains completely insensitive to the effects of eIF2 phosphorylation.

phenotype only partially suppressed the Slg$^-$ phenotype and were resistant to 3AT in the *GCN2^c-513* strain (Fig. 2C). Overexpression of the mammalian eIF2α kinase PKR in place of GCN2 is lethal in yeast due to extreme levels of eIF2α phosphorylation on Ser-51 (8, 15). Suppression of this lethality was used as another means of ranking the *GCD2* mutations. Again, the three mutants that exhibited the strongest Gcn$^-$ phenotypes in the strains containing the *GCN2^c* alleles also were the most effective in suppressing the lethal effects of PKR overexpression. Indeed, the *GCD2-L381Q* and *-K627T* alleles completely overcame the toxicity of PKR expression, as they grew indistinguishably from an isogenic strain with the alanine-51 substitution in eIF2α (Fig. 2C). These last results suggested that the L381Q and K627T substitutions in GCD2 make eIF2B completely insensitive to eIF2α phosphorylation. The E377K substitution is slightly less effective, and the other six mutations are considerably less effective than are L381Q and K627T in overcoming the inhibitory effects of eIF2(αP) on eIF2B recycling activity.

Regulatory mutations in *GCD7* and *GCN3* alter residues in segments homologous to GCD2. The mutational analysis described above identified three regions in the C-terminal half of GCD2 with an important role in negative regulation of eIF2B by eIF2(αP). We considered the possibility that homologous segments in GCD7 and GCN3 would also be involved in the regulatory functions of eIF2B. To test this hypothesis, we isolated point mutations in *GCN3* and additional mutations in *GCD7* as suppressors of *GCN2^c-516*, to compare the locations of a large number of regulatory substitutions obtained in the three different proteins.

A low-copy-number *GCD7* plasmid was mutagenized in a bacterial mutator strain and introduced into a *gcd7Δ GCN2^c-516* strain by plasmid shuffling. The resulting strains were screened for reversion of the Slg$^-$ phenotype of the *GCN2^c-516* allele. We obtained 11 novel suppressor alleles and characterized them in parallel with the *GCD7* regulatory alleles described previously (47) by the genetic tests used as described above to rank the *GCD2* suppressors (Fig. 3). One of the new suppressors, *GCD7-S119P*, resembled the *GCD2-L381Q* and *GCD2-K627T* alleles, conferring complete insensitivity to eIF2 phosphorylation. Previously, this extreme phenotype was achieved for *GCD7* only by combining two mutations, *GCD7-1118T,D178Y* (Fig. 3) (47). All of the *GCD7* regulatory mutations alter amino acids within regions of sequence similarity in GCD7, GCD2, and GCN3, with none occurring in the unconserved N-terminal 65 residues of GCD7 (Fig. 3A). In addition, eight of the complete set of 15 *GCD7* suppressors (substitutions *P291S*, *V292A*, *Y305C*, *P306I*, *K329E*, *I348V*, *N357I*, and *S359G*) mapped within, or just upstream of, the highly conserved C-terminal domain (Fig. 3A), verifying the

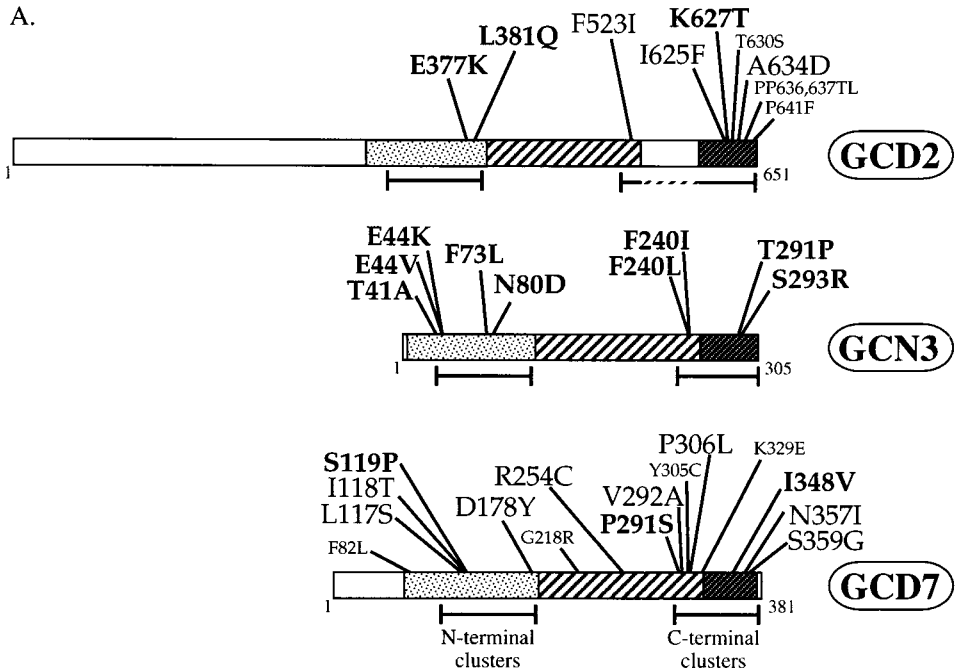

FIG. 5. Alignment of eIF2B sequences, showing the locations of regulatory mutations. (A) The protein-coding sequences of GCD2, GCN3, and GCD7 are depicted as in Fig. 1 with the addition of all of the regulatory mutations described in Fig. 2, 3, and 4. Horizontal bars indicate the ca. 70-amino-acid intervals containing the N- and C-terminal clusters of regulatory mutations for each protein. The GCD2 C-terminal cluster is interrupted by a 51-residue stretch with no homology to GCN3 or GCD7. (B and C) Multiple sequence alignment of eIF2B proteins. Three eIF2Bα sequences (rat, *C. elegans*, and yeast) were aligned with two eIF2Bβ sequences (human and yeast) and two eIF2Bδ sequences (rat and yeast). Two parts of the alignment, containing the N-terminal (B) and C-terminal (C) clusters of mutations, are shown. Residues mutated in the yeast subunits are indicated, with the substituting amino acid in the mutant shown directly below. In addition, pound symbols (#) directly above each row of the alignment highlight the clustering of these mutated residues. Gaps introduced into the alignment are shown with dots, and nonsense codons are shown with asterisks. Boxes indicate residues identical in at least five of the seven sequences. Conservative substitutions in at least five of seven residues are shaded.

importance of this region in the regulatory functions of both GCD7 and GCD2. Five mutations in *GCD7* (*F82L*, *L117S*, *I118T*, *S119P*, and *D178Y*) were located in the N-terminal region of similarity with GCD2 (Fig. 3A), where the *E377K* and *L381Q* mutations in *GCD2* mapped, indicating the importance of this region also for the regulatory functions of both subunits.

To confirm that the phenotypes of the mutations that we isolated in *GCD2* and *GCD7* were not caused by variations in the levels of the subunits of eIF2B, we used immunoblot analysis to analyze the steady-state levels of GCD2, GCD6, GCD7, and GCN3 in strains containing each of the suppressor alleles. We observed no significant variations from the wild-type levels of these proteins in any mutant (data not shown).

Error-prone PCR mutagenesis of *GCN3* and screening of mutagenized plasmids for dominant suppression of the Slg$^-$ phenotype of a *GCN3 GCN2^c-516* strain was used to isolate dominant suppressors in *GCN3*. In this case, only the fastest-growing revertants were selected for analysis. The resulting nine alleles contained single-codon substitutions in *GCN3* that displayed a pattern of clustering similar to that seen for the *GCD2* and *GCD7* mutations (Fig. 4A). These alleles were characterized by the genetic tests used to rank *GCD2* and *GCD7* suppressors (Fig. 4). All nine *GCN3* suppressors resembled *GCD2-L381Q*, *GCD2-K627T*, and *GCD7-S119P* in completely overcoming the growth defects associated with eIF2α phosphorylation. This was surprising because even deletion of *GCN3* does not completely overcome the toxicity of PKR overexpression in yeast cells. Thus, single amino acid changes in GCN3 can make eIF2B less sensitive to eIF2(αP) than does removing GCN3 from the complex.

Regulatory mutations cluster within two segments in each subunit. The relative positions of the suppressor mutations that we isolated in *GCD2*, *GCD7*, and *GCN3* are summarized in Fig. 5A. With the exception of three substitutions in *GCD7* (*F82L*, *G218R*, and *R254C*), all other mutations map in either of two segments of *GCD2*, *GCD7*, and *GCN3*. A ca. 70-residue segment located at the highly conserved C terminus of each protein encompasses seven of the nine mutations in GCD2 and roughly half of the mutations in GCD7 and GCN3 (Fig. 5A). This segment in GCD2 is interrupted by a 51-amino-acid region of nonhomology. The rest of the mutations fall into a second ca. 70-residue segment located near the N-terminal boundary of the region of shared homology in each protein (Fig. 5A). These observations suggest that homologous structural elements in GCD2, GCD7, and GCN3 mediate the regulatory functions of these proteins and imply that the regulatory functions of GCD2, GCD7, and GCN3 are closely related.

To investigate whether any of the suppressor mutations alter equivalent positions in the homologous segments of GCD2, GCD7, and GCN3, we constructed a multiple sequence alignment of the yeast eIF2B subunits and their homologs in *C. elegans* and mammalian species. Figure 5B and C display two sections from this alignment encompassing the N-terminal and C-terminal clusters of regulatory mutations, respectively. We found that suppressors mapping in the C-terminal clusters (Fig. 5C) had substituted residues at equivalent positions in GCD2 and GCD7 (*GCD7-I348V* and *GCD2-K627T*), in GCD7 and GCN3 (*GCD7-S359G* and *GCN3-S293R*), or even in all three subunits (*GCN3-T291P*, *GCD7-N357I*, and *GCD2-P636T*) (Fig. 5C). In addition, *GCD2-F523I* and the *Y305C* and *P306L* mutations in *GCD7* are only several residues away from

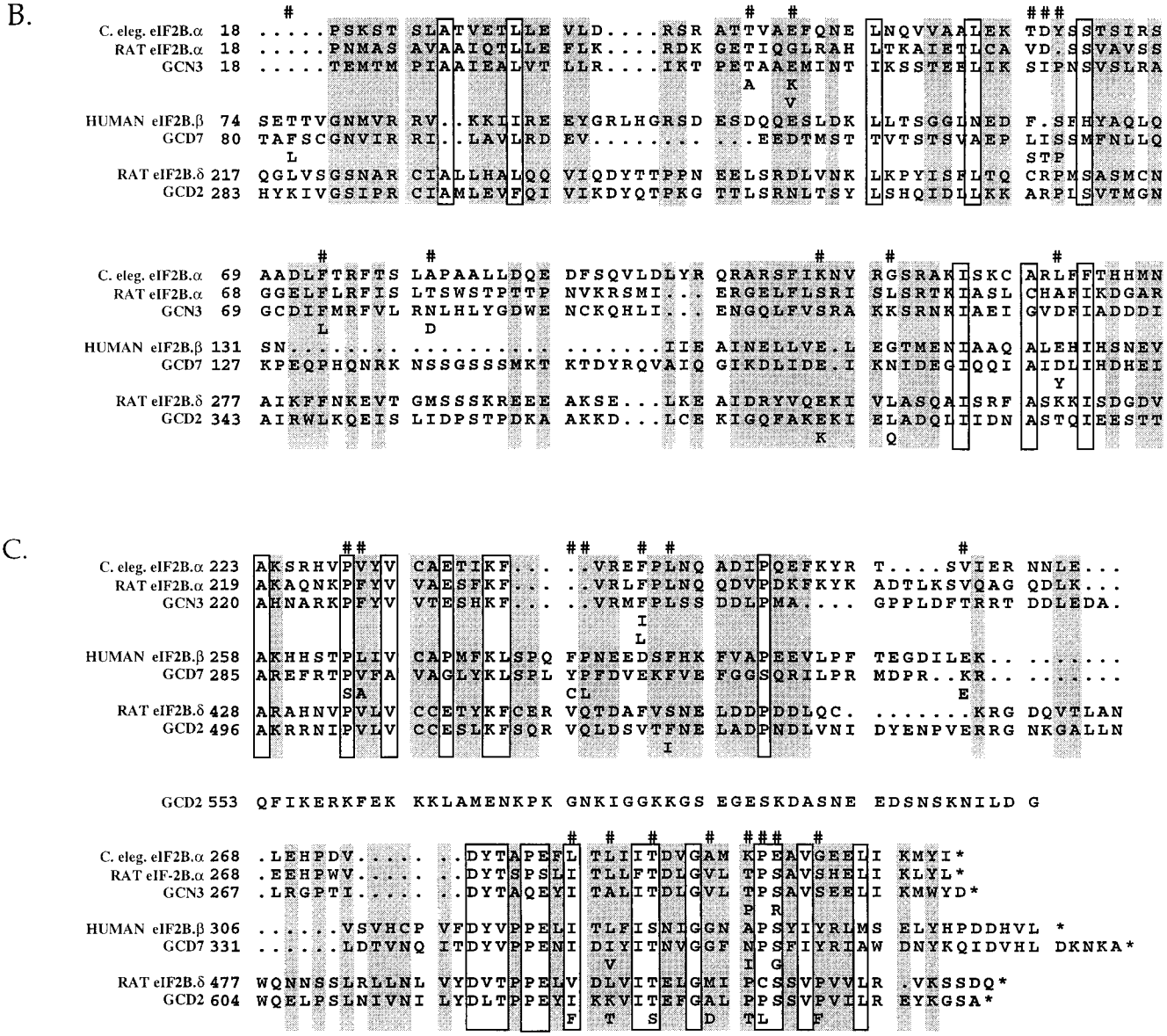

FIG. 5—*Continued.*

the *F240I* and *F240L* changes in *GCN3*. These results indicate that certain positions in the extreme C-terminal domains of all three subunits carry out critical regulatory functions, providing further evidence that these regions are both structurally and functionally related.

Many critical regulatory residues are located at unique positions within the homologous segments. Although several of the regulatory substitutions in the C-terminal clusters altered equivalent positions in the three proteins (Fig. 5C), this was not true of others in this segment, nor did it apply to any of the suppressor mutations in the N-terminal clusters. Figure 5B shows that the mutations in the latter region form four independent clusters separated from each other by 12 to 26 residues. Thus, all of the critical residues identified in the N-terminal conserved segments are at unique positions in each subunit. It was conceivable that our mutagenesis experiments did not saturate the regulatory sites in these proteins and that equivalent positions are actually critical for regulation more frequently than our results indicate. In an effort to rule out this possibility, we pursued the fact that suppressors were obtained which alter identical residues at the same positions in the C-terminal segment of GCD7 at Ser-359 and in GCN3 at Ser-293, whereas none were isolated at the corresponding position in GCD2 (Ser-638). If this occurred because the mutagenesis of *GCD2* was not saturating, then alteration of Ser-638 in GCD2 should have a suppressor phenotype. To test this prediction, we used site-directed mutagenesis to replace Ser-638 in GCD2 either with Arg, the nonconservative replacement at the homologous position in *GCN3-S293R* (Fig. 5C), or with Cys. In parallel, we altered Pro-502 in GCD2 to Ser because the homologous Pro residue had been altered in *GCD7-P291S* and also because this is the only residue altered in one of our suppressors that is invariant among GCD2, GCD7, GCN3, and their homologs in higher eukaryotes (Fig. 5C). As described next, neither *GCD2* mutation had the suppressor phenotype.

A.

Relevant Genotype	*GCD2* Allele:								
	GCD2			*gcd2*-S638R			*gcd2*- P502S		
	SD	3AT	5FT /TRA	SD	3AT	5FT /TRA	SD	3AT	5FT /TRA
gcd2Δ	5+	3+	+/-	2+	3+	3+	5+	3+	+/-
gcd2Δ, gcn2Δ	5+	0	n.d.	2+	3+	n.d.	5+	0	n.d.
gcd2Δ, gcn3Δ	5+	0	n.d.	5+	0	n.d.	5+	0	n.d.

B.

Transformed *GCN2* allele.	*GCD2* Allele:			
	GCD2		*gcd2*- P502S	
	SD	3AT	SD	3AT
Vector	5+	0	5+	0
GCN2	5+	3+	5+	3+
GCN2^c-516	2+	3+	+/-	n.d.
GCN2^c-513	1+	2+	-/+	n.d.
gcn2-507	5+	+/-	5+	1+

C.

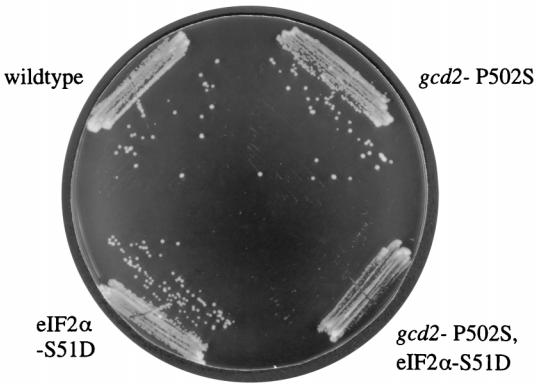

FIG. 6. Site-directed mutagenesis reveals different functions for equivalent positions in *GCD2*, *GCD7*, and *GCN3*. (A) Plasmids bearing wild-type *GCD2* (pAV1026), *gcd2-S638R* (pAV1104), or *gcd2-P502S* (pAV1102) were introduced by plasmid shuffling into strains with *GCD2* alone deleted (*gcd2*Δ; strain GP3040) or also lacking *GCN2* (*gcd2*Δ *gcn2*Δ; strain GP3224) or *GCN3* (*gcd2*Δ *gcn3*Δ; strain GP3160). The resulting transformants were analyzed for growth defects by streaking for single colonies on SD medium containing the appropriate supplements and by replica plating to the same medium supplemented with 3AT, as described in the legend to Fig. 2C. Replica plating to SD medium supplemented with 5-fluorotryptophan and 1,2,4-triazoleanaline was also measured, with the maximum growth rate scored as 3+. Growth differing from that of the wild-type *GCD2* strain is shown shaded. n.d., not determined. (B) Strain GP3224 (*gcd2*Δ *gcn2*Δ) bearing *GCD2* or *gcd2-P502S* was transformed with one of the following plasmid-borne alleles of *GCN2* or with empty vector (p713): wild-type *GCN2* (p722), *GCN2^c-516* (p1056), *GCN2^c-513* (p1052), or *GCN2-507* (p561). Growth was assessed as described in the legend to Fig. 2C, and key results are shaded. (C) Derivatives of GP3514 (*gcd2*Δ *sui2*Δ *gcn2*Δ) containing *GCD2*, *gcd2-P502S*, and plasmid-borne *SUI2* alleles encoding wild-type eIF2α (p1097) or eIF2α-S51D (p1101) were streaked for single colonies on minimal medium supplemented with uracil (SD) and grown for 2.5 days at 30°C.

The *gcd2-S638R* mutation led to a Slg$^-$ phenotype under nonstarvation conditions in an otherwise wild-type strain and conferred resistance to 3AT in a *gcn2*Δ background (Fig. 6A). These phenotypes are characteristic of recessive *gcd* mutations, which are thought to reduce the catalytic activity of eIF2B. *gcd2-S638R* also conferred increased resistance to the amino acid analogs 5-fluorotryptophan and 1,2,4-triazolealanine, additional phenotypes of *gcd* mutations resulting from constitutive derepression of *GCN4* and its target enzymes in the tryptophan and histidine biosynthetic pathways. Interestingly, both the Gcd$^-$ and Slg$^-$ phenotypes of the *gcd2-S638R* allele were expressed only when GCN3 was present in the cell. Thus, deletion of *GCN3* in the *gcd2-S638R* strain conferred growth rates on SD and SD-3AT medium identical to those observed in the isogenic *GCD2 gcn3*Δ strain (Fig. 6A). Nearly identical results were obtained when Ser-638 in GCD2 was changed to cysteine (data not shown). Interestingly, GCN3 appears to be maintained in the eIF2B complex even though its inclusion facilitates the deleterious effects of the Ser-638 substitutions in GCD2 on the cellular growth rate.

The *gcd2-P502S* allele also did not exhibit the regulatory phenotype observed for the homologous substitution in *GCD7* (*P291S*). Our initial genetic analysis revealed no phenotypic differences between this mutant allele and wild-type *GCD2* (Fig. 6A). Upon further analysis, however, we observed phenotypes consistent with the idea that the P502S substitution in GCD2 makes eIF2B hypersensitive, rather than insensitive, to eIF2 phosphorylation. *gcd2-P502S* had no detectable effect on growth under nonstarvation conditions in wild-type *GCN2* cells, but it exacerbated the Slg$^-$ phenotype of the *GCN2^c-516* and *GCN2^c-513* alleles under the same conditions (Fig. 6B). Although *gcd2-P502S* had no effect on 3AT sensitivity in a *gcn2*Δ strain, it increased 3AT resistance in the *gcn2-507* background. The *gcn2-507* allele encodes a protein kinase that phosphorylates eIF2α at reduced levels under histidine starvation conditions, causing reduced growth on 3AT medium (49). The partial restoration of growth on 3AT medium in the *gcn2-507* strain plus the exacerbation of the slow growth in the *GCN2^c* strains can be explained if this mutant eIF2B is inhibited more effectively than wild-type eIF2B by phosphorylated eIF2. As a further test of this idea, we examined genetic interactions between *gcd2-P502S* and mutations in eIF2α at the phosphorylation site, serine-51. As expected, the *gcd2-P502S* allele had no phenotype in the strain containing wild-type or the Ala-51 mutant of eIF2α. In contrast, combining *gcd2-P502S* with the Asp-51 form of eIF2α significantly reduced growth on SD medium (Fig. 6C [Ala-51 not shown]). We showed previously that eIF2α-S51D mimics phosphorylation of Ser-51 in vivo by eliciting partial derepression of *GCN4* translation (16). Thus, the synergistic growth defect seen when eIF2α-S51D is combined with the *gcd2-P502S* product is also consistent with the idea that eIF2B containing P502S in GCD2 is hypersensitive to phosphorylated eIF2.

In conclusion, none of the *GCD2* alleles constructed by site-directed mutagenesis exhibited the suppressor phenotype. Therefore, although the suppressor mutations cluster in homologous segments in GCD2, GCD7, and GCN3, many positions in these segments that are critically required for regulation differ among the three proteins.

The regulatory mutations do not exclude GCN3 from eIF2B. Deletion of *GCN3* makes the resulting four-subunit eIF2B complex less sensitive to eIF2 phosphorylation (Fig. 4B and 6A). It was possible, therefore, that the regulatory mutations we isolated in *GCD2*, *GCD7*, and *GCN3* exert their effects primarily by excluding GCN3 from eIF2B. Several genetic observations suggested that this was not true. For the *GCN3* suppressors, all of the mutations are dominant over the wild-type allele, implying that the mutant proteins are replacing wild-type GCN3 in the eIF2B complex. Second, high-level expression of PKR in yeast is lethal, and deletion of *GCN3* only partially overcomes this lethality, resulting in a Slg$^-$ phenotype

A.

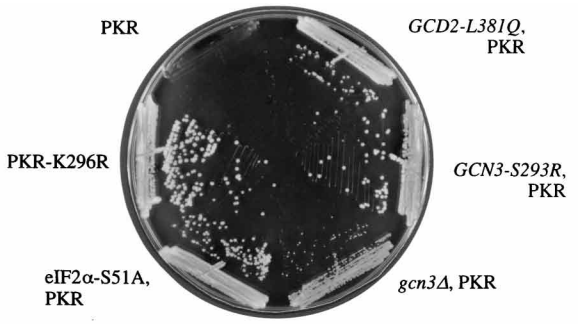

B.

GCD2 Allele	Relevant genotype		
	GCN3	*gcn3Δ*	
	PKR	*GCN2*	PKR
	SGAL	3AT	SGAL
GCD2	0	0	2+
Class I			
E377K	3+	1+	2+
L381Q	4.5+	0	2+
K627T	4.5+	0	2+
Class II			
T630S	+/-	0	3+
P636T,P637L	+/-	0	3+
P641F	-/+	0	3+
Class III			
F523I	1+	0	2+
A634D	1.5+	0	2+

C.

GCD7 Allele	Relevant genotype		
	GCN3	*gcn3Δ*	
	+ PKR	*GCN2*	+ PKR
	SGAL	3AT	SGAL
GCD7	0	0	2+
Class I			
S119P	4.5+	0	2+
I118T, D178Y	4.5+	0	2+
V292A	1+	2+	1+
I348V	3+	3+	n.d.
Class II			
D178Y	1+	0	4.5+
G218R	+/-	0	3+
R254C	2+	0	3+
N357I	1+	0	3+
Class III			
F82L	+/-	0	2+
L117S	1+	0	2+
I118T	2+	0	2+
P291S	3+	0	3+
Y305C	+/-	0	2+
P306L	1+	0	2+
K329E	-/+	0	2+
S359G	2+	0	2+

FIG. 7. Genetic evidence that mutations in *GCD2* and *GCD7* do not exclude GCN3 from eIF2B. (A) Suppression of the toxicity of overexpressing PKR in yeast by mutations affecting eIF2B subunits. Transformants of isogenic strains bearing the PKR cDNA with the *GAL10-CYC* promoter, selected from those shown in Fig. 2 and 4, were streaked for single colonies on minimal galactose medium (SGAL) and grown for 7 days at 30°C in parallel with the following control strains: (i) a transformant of GP3224 (*gcd2*Δ *gcn2*Δ) containing the plasmid-borne cDNA encoding the catalytically defective mutant PKR-K296R (p1421) and (ii) strain H1645 (*sui2*Δ) containing plasmids encoding eIF2α-S51A (p1098) and wild-type PKR (p1420). (B) Effects of deleting *GCN3* on phenotypes of *GCD2* regulatory mutants. Strains GP3224 (*gcd2*Δ *GCN3*), GP3160 (*gcd2*Δ *gcn3*Δ), and GP3160 containing p1420 encoding PKR were transformed with plasmids bearing the indicated *GCD2* alleles. Growth of the resulting transformants was assessed as described in the legend to Fig. 2C. The three categories of mutations (classes I, II, and III) are described in the text. (C) Effects of deleting *GCN3* on phenotypes of *GCD7* mutants. Phenotypic analysis identical to that shown in panel B was performed for *GCD7* mutants by using transformants of strains H2218 (*gcd7*Δ *GCN3*) and H2220 (*gcd7*Δ *gcn3*Δ). n.d., not determined.

(Fig. 4B and 7A). In contrast, all of the *GCN3* suppressors (Fig. 4B) and several mutations in *GCD2* (*E377K*, *L381Q*, and *K627T*) (Fig. 7A and B) and *GCD7* (*S119P*, *P291S*, and *I348V*) (Fig. 7C) completely overcame the toxicity of PKR expression. These results provide strong evidence that all of the products of the *GCN3* suppressors are stable components of the eIF2B complex in vivo. Moreover, elimination of GCN3 from eIF2B, even if it occurs, cannot be the sole reason why eIF2B is resistant to eIF2(αP) in strains containing the most potent *GCD2* and *GCD7* suppressors.

A third argument that the *GCD2* and *GCD7* suppressors do not simply cause GCN3 to dissociate from eIF2B is that the phenotype of many suppressor alleles is actually dependent on the presence of *GCN3*. We made this observation by examining the ability of each *GCD2* and *GCD7* suppressor to overcome the toxicity of PKR overexpression in a pair of isogenic *GCN3* and *gcn3*Δ strains. Based on the results shown in Fig. 7B and C, the suppressors were placed in three different classes. Class I contains mutations that overcome the toxicity of eIF2(αP) more effectively in the *GCN3* strain than in the *gcn3*Δ mutant. This behavior was observed for the three most efficient *GCD2* suppressors (*GCD2-E377K*, *-L381Q*, and *-K627T*) and for the two most effective *GCD7* suppressors (*GCD7-S119P* and *-I118T,D178Y*). For example, the *GCD2-K627T* and *GCD7-S119P* alleles fully suppressed the toxicity of PKR overexpression in the *GCN3* strain but appeared to have no phenotype in the isogenic *gcn3*Δ strain, with the double mutants exhibiting the same Slg$^-$ phenotype seen in the *GCD2 gcn3*Δ and *GCD7 gcn3*Δ strains overexpressing PKR (Fig. 7B and C). The other two mutations placed in this class show more extreme changes in the *gcn3*Δ strain. *GCD7-I348V*, and to a lesser extent *GCD7-V292A*, grow slowly on minimal SD medium when combined with *gcn3*Δ (not shown), and they also grow on 3AT-containing medium (Fig. 7C). This implies that when these mutations in *GCD7* and *gcn3*Δ are combined, the eIF2B complexes formed have reduced catalytic activity. Because the mutations in class I suppress the toxic effects of eIF2(αP) in the presence of *GCN3* but not in its absence, it is highly unlikely that they exert their effects by excluding GCN3 from eIF2B.

All of the suppressor mutations in class II only partially suppressed the lethality of PKR in the *GCN3* background, and suppression by these mutations was enhanced by deletion of *GCN3*. Thus, the level of suppression observed for the class II mutations in the *gcn3*Δ background was greater than that conferred by *gcn3*Δ alone (Fig. 7B and C). The additive effects of combining these *GCD2* or *GCD7* suppressors with *gcn3*Δ implies that the class II substitutions act independently of GCN3 rather than by excluding GCN3 from the complex.

The class III mutations are not dependent on *GCN3* for suppression and do not have an additive effect when combined with *gcn3*Δ. With the exception of *GCD7-P291S*, the mutations in this class suppress PKR toxicity in the *GCN3* strain less than the *gcn3*Δ mutation does, and they produce no additional suppression when combined with *gcn3*Δ. The fact that these mutations are phenotypically silent in a *gcn3*Δ strain could indicate that they act primarily by reducing the amount of GCN3 stably associated with the eIF2B complex. However, because *GCD7-P291S* suppresses PKR toxicity more effectively than does *gcn3*Δ, exclusion of GCN3 from eIF2B cannot be the sole mechanism of suppression for this mutation; indeed, biochemical evidence (described below) shows that for this and other mutants, GCN3 remains stably associated with eIF2B.

With the exception of suppressors in class III, the genetic interactions just described strongly suggest that these mutations do not exclude GCN3 from eIF2B as the primary means of decreasing sensitivity to eIF2(αP). To obtain physical evidence supporting this conclusion, coimmunoprecipitation experiments were performed to evaluate the relative amounts of GCN3 that are complexed with the GCD6 subunit of eIF2B in the suppressor mutants. We have shown previously that antibodies against GCD6 specifically and quantitatively coimmunoprecipitate all five subunits of eIF2B from cell extracts (6). For our studies, we selected three *GCD2* and three *GCD7* mutants, representing each class of suppressors identified by the genetic analysis described above (Fig. 7). From the data shown in Fig. 8, it can be seen that GCN3 was equally coimmunoprecipitated with GCD6 from high-salt extracts of pelleted ribosomes prepared from the mutant and wild-type strains. These results show that the *GCD2* and *GCD7* suppres-

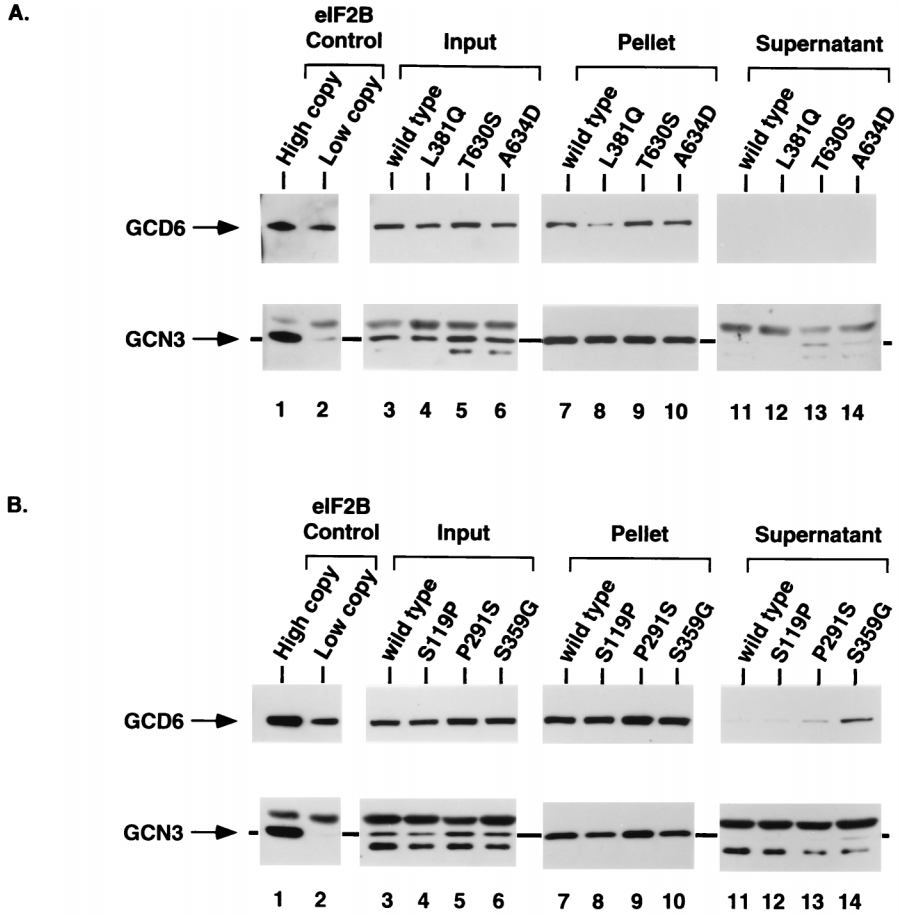

FIG. 8. Coimmunoprecipitation of GCN3 with GCD6 from strains bearing regulatory mutations in *GCD2* or *GCD7*. (A) RSW fractions were prepared from strain GP3040 (*gcd2*Δ) containing the following *GCD2* alleles: wild-type *GCD2* (pAV1026), *GCD2-L381Q* (pAV1031), *GCD2-T630S* (pAV1034), and *GCD2-A634D* (pAV1035). eIF2B complexes were immunoprecipitated from these fractions by using polyclonal antiserum raised against the GCD6 subunit of eIF2B. Eighty-three micrograms of RSW (Input), the coimmunoprecipitation pellets obtained from 166 μg of RSW, and the supernatants remaining after immunoprecipitation from 83 μg of RSW were separated by sodium dodecyl sulfate–10% polyacrylamide gel electrophoresis, blotted to nitrocellulose, and probed with rabbit polyclonal sera against eIF2B subunits as described previously (6, 10, 11). Bound antiserum was detected by using horseradish peroxidase-linked protein A and enhanced chemiluminescence. Staining of nitrocellulose membranes with Ponceau S (Sigma) showed that the coimmunoprecipitations were specific, as all visible input proteins were retained in the supernatant fractions. For simplicity, only the coimmunoprecipitation of GCN3 with GCD6 is shown; however, GCD1, GCD2, and GCD7 were found to be distributed between pellet and supernatant fractions similarly to GCN3 and GCD6. Whole-cell extracts from yeast strains with eIF2B subunits on low- or high-copy-number plasmids (prepared as described in reference 17) were analyzed in parallel to identify unambiguously each immunoreactive species. (B) Same as for panel A except that transformants of strain H2217 (*gcd7*Δ) bearing the following plasmids containing the indicated *GCD7* alleles were analyzed: *GCD7-S119P* (pAV1079), *GCD7-P291S* (pAV1083), and *GCD7-S359G* (pAV1088). Identical control immunoprecipitation reactions with 10 μl of GCD6 preimmune serum failed to precipitate any eIF2B proteins (data not shown) (6).

sor mutations in these six strains do not act by excluding GCN3 from eIF2B and confirm our interpretation of the genetic data in Fig. 7. We conclude that GCD2, GCD7, and GCN3 each play a direct role in the regulation of eIF2B activity by phosphorylated eIF2 and that a single missense change in any one of these three subunits is sufficient to disrupt the regulatory mechanism.

eIF2α is highly phosphorylated in eIF2B mutants expressing PKR. It was conceivable that the suppressor mutations overcome the toxicity of *GCN2*^{c} alleles and PKR expression by decreasing the level of eIF2α phosphorylation. Therefore, we examined eIF2α phosphorylation in *GCD2* mutant strains by using isoelectric-focusing gel electrophoresis of whole-cell extracts followed by immunoblot analysis with eIF2α-specific antiserum. When PKR expression was induced in the wild-type *GCD2* strain, a portion of eIF2α became phosphorylated in a manner that was completely dependent on PKR and Ser-51 in eIF2α, being abolished by the K296R substitution in PKR or the Ala-51 substitution in eIF2α (Fig. 9, lanes 1, 2, and 11). We showed previously that the L84F substitution in eIF2α, which renders eIF2(αP) impotent as an inhibitor of eIF2B, leads to a higher level of eIF2(αP) in vivo than occurs in isogenic wild-type eIF2α cells (Fig. 9, lanes 1 and 12) (46). This increase in the level of eIF2(αP) appears to result from increased expression of PKR under conditions where eIF2α phosphorylation does not inhibit translation initiation (36). We observed the same phenomenon for the *GCD2* suppressors; moreover, the percentage of eIF2α phosphorylation correlated with the degree of suppression of PKR toxicity by the different mutations (Fig. 9, lanes 3 to 10, and Fig. 2). These results, together with similar findings for *GCD7* suppressors (47) and for *gcn3*Δ (15), confirm that the regulatory mutations do not overcome the toxicity of PKR by reducing phosphorylation of eIF2α. Moreover, the fact that ca. 80% of the eIF2α is phosphorylated in the *GCD2-L381Q* and *GCD2-K627T* suppressor strains suggests that these two mutations, and perhaps others, allow

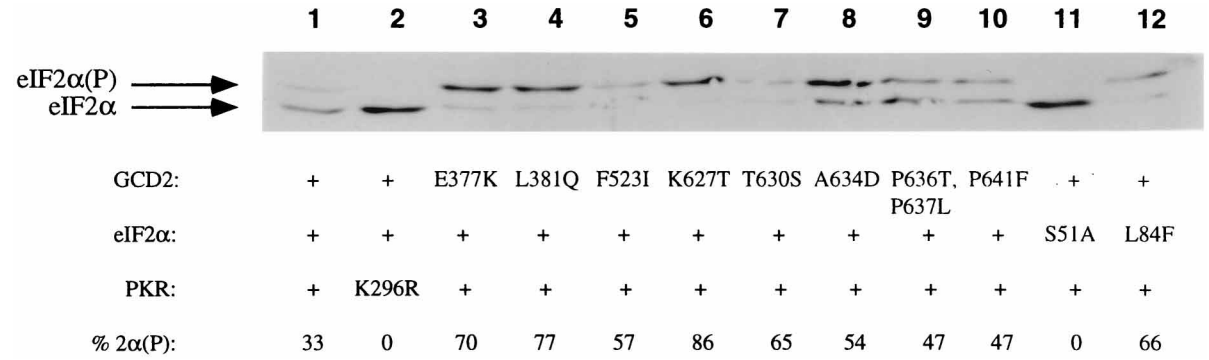

FIG. 9. Isoelectric-focusing gel electrophoresis of eIF2α from *GCD2* mutant strains expressing PKR. Derivatives of strain GP3224 (*gcd2*Δ *gcn2*Δ) with the plasmid-borne wild-type or the indicated mutant *GCD2* allele and strain H1645 (*sui2*Δ) with plasmid-borne *SUI2* alleles encoding eIF2α-S51A (p1098) or eIF2α-L84F (p1350) were transformed with a plasmid encoding PKR (p1420) or the catalytically inactive PKR-K296R allele (p1421). The resulting strains were grown in minimal raffinose medium for 24 h, and galactose was added to induce expression of PKR for an additional 14 hours. Samples of total cellular protein were separated by isoelectric focusing on a one-dimensional vertical slab gel followed by immunoblot analysis with antibodies against eIF2α. The eIF2α antiserum reacts equally well with both the basal and hyperphosphorylated (more acidic) species, as they were raised to a C-terminal fragment of eIF2 lacking Ser-51 (16). Relevant genotypes are shown, where + indicates the wild-type gene. The percentage of the total eIF2α immunoreactivity found in the species phosphorylated on Ser-51 [% 2α(P)] was determined by quantitative densitometry.

eIF2B to catalyze nucleotide exchange on phosphorylated eIF2.

DISCUSSION

Homologous segments in GCD2, GCD7, and GCN3 function in the regulation of eIF2B by phosphorylated eIF2. eIF2B is unique among guanine nucleotide exchange factors in being regulated by phosphorylation of its substrate, eIF2. Experiments with purified mammalian factors have shown that eIF2(αP) · GDP acts as an inhibitor of eIF2B, preventing the recycling of nonphosphorylated eIF2 · GDP to eIF2 · GTP. We previously proposed that regions of sequence homology shared by three of the eIF2B subunits, GCN3, GCD7, and the C-terminal half of GCD2, all function in this regulatory step (22). This idea was based on the fact that deletion of *GCN3* appears to make eIF2B less sensitive to eIF2(αP) and on the isolation of several *GCD7* point mutations with the same phenotype. The results presented in this report provide strong support for this hypothesis and identify particular segments in the homologous regions of GCD2, GCD7, and GCN3 that are critically required for their regulatory functions.

We have isolated 29 novel mutations in *GCD2*, *GCD7*, and *GCN3* that reduce or abolish the response to eIF2(αP) without causing an apparent defect in eIF2B catalytic activity. These regulatory mutations are not distributed randomly throughout each subunit. First, all of the *GCD2* suppressors map in the C-terminal half of the protein, which is homologous to GCD7 and GCN3. Second, almost all of the regulatory mutations are clustered in two segments of ca. 70 amino acids in each subunit, located at the amino and carboxyl ends of the region of sequence similarity (Fig. 5A). Several substitutions in the C-terminal clusters of mutations alter residues at equivalent positions in two of the three subunits or even in all three proteins (Fig. 5C). The fact that homologous segments, and even identical amino acid positions, in GCD2, GCD7, and GCN3 are critically required for inhibition of eIF2B by eIF2(αP) implies that structurally similar elements in these proteins carry out related functions in the regulatory mechanism. As described below, we propose that these three subunits form a single regulatory domain in eIF2B, which makes multiple contacts with eIF2α around the site of phosphorylation at Ser-51, allowing eIF2B to sense and respond to eIF2α phosphorylation.

GCD2, GCD7, and GCN3 make independent contributions to the regulation of eIF2B by eIF2(αP) as components of a single regulatory domain. The fact that single mutations were obtained in *GCD2*, *GCD7*, and *GCN3*, each of which abolishes negative regulation of eIF2B by eIF2(αP), suggests that all three proteins play critical roles in the regulatory mechanism. However, it could be imagined instead that the mutations in *GCD2* and *GCD7* impair regulation indirectly by affecting the function of GCN3. One way that this might occur is for mutations in *GCD2* or *GCD7* to cause dissociation of GCN3 from the eIF2B complex. This possibility was eliminated for most of the regulatory mutations we isolated by a combination of genetic and biochemical experiments. The coimmunoprecipitation data in Fig. 8 showed that GCN3 was present at normal levels in the eIF2B complexes found in a number of strains containing different *GCD2* and *GCD7* suppressors analyzed by this technique. In addition, genetic experiments showed that the regulatory effects of several *GCD2* and *GCD7* mutations (designated class I alleles) are greatly dependent on the presence of *GCN3* (Fig. 7), indicating that GCN3 resides in these mutant eIF2B complexes. The ability of other *GCD2* and *GCD7* mutations (designated class II alleles) to suppress the toxicity of eIF2(αP) was enhanced by deletion of *GCN3*. The fact that the phenotypes of the class II *GCD2* and *GCD7* mutations are additive with *gcn3*Δ provides strong evidence that GCD2 and GCD7 contribute to the regulation of eIF2B independently of GCN3.

Previously, we observed numerous allele-specific interactions between mutations in *GCD2* and *GCN3*, which suggested that these two subunits contact one another in eIF2B (6). We recently provided biochemical evidence confirming that GCD2, GCD7, and GCN3 physically interact with one another and comprise a regulatory domain in eIF2B. Cooverexpression of these three subunits specifically reduced the growth-inhibitory effects of eIF2α phosphorylation in vivo. The excess subunits present in the overproducing strains were assembled into a stable subcomplex lacking GCD1 and GCD6 that could be immunoprecipitated from yeast cells. Genetic experiments indicated that the overexpressed GCD2-GCD7-GCN3 subcomplex did not possess eIF2-recycling activity, suggesting that it functioned to sequester eIF2(αP) and rescue the native eIF2B complex from the inhibitor (52). In addition, formation of this subcomplex did not require the amino-ter-

minal half of GCD2, the region lacking sequence similarity with GCD7 and GCN3. Combining these results with the present findings leads us to propose that GCD2, GCD7, and GCN3 constitute a regulatory domain in eIF2B which interacts with eIF2α in the region of the phosphorylation site. This provides an explanation for why a single missense mutation in only one of these subunits can abolish the regulatory mechanism (Fig. 2 to 4). Regions of homology in the three subunits that are largely devoid of regulatory mutations are hydrophobic and so may comprise the structural cores of these proteins or mediate their interactions with other subunits in the eIF2B complex.

Genetic evidence supports the idea that the eIF2B regulatory domain directly interacts with eIF2α in the vicinity of Ser-51. It was found that the L84F substitution in eIF2α, which eliminated the growth-inhibitory effect of phosphorylated eIF2 (46), also suppressed the impairment of eIF2B function caused by a subset of *gcn3*^{c} alleles (47). As GCN3 is dispensable for catalysis, it is improbable that the *gcn3*^{c} alleles directly impair the active site for nucleotide exchange in eIF2B. It seems more likely that they alter the interaction between eIF2 and eIF2B in a way that mimics the inhibitory effect of eIF2(αP). If so, they may cause nonphosphorylated eIF2 · GTP to dissociate more slowly from eIF2B, decreasing the amount of eIF2B that is available to bind eIF2 · GDP. Interestingly, the *gcn3*^{c} alleles that are efficiently suppressed by the eIF2α-L84F substitution (*gcn3*^{c}*-A26T*, *gcn3*^{c}*-D71N*, and *gcn3*^{c}*-R104K*) all map within the N-terminal cluster of Gcn$^-$ alleles in *GCN3* described here (Fig. 5), consistent with the idea that this ca. 70-residue segment of GCN3 directly interacts with eIF2α.

A model for nucleotide exchange and its inhibition by phosphorylated eIF2. A critical question regarding the mechanism of guanine nucleotide exchange by eIF2B and its inhibition by eIF2(αP) is whether the regulatory domain of eIF2B constituted by GCD2, GCD7, and GCN3 interacts with both eIF2 and eIF2(αP). If the regulatory domain of eIF2B interacted only with the inhibitor eIF2(αP), this would imply the existence of two distinct binding sites for eIF2 on eIF2B, one catalytic and one regulatory. In this model, the substrate eIF2 would have a high affinity for the catalytic site but a low affinity for the regulatory site, while the reverse would be true for the inhibitor, eIF2(αP). In addition, binding of the inhibitor to the regulatory site would have to prevent either binding or nucleotide exchange of the substrate at the catalytic site. A simpler idea is that eIF2 and eIF2(αP) bind at the same location on eIF2B, with different eIF2B subunits making distinct contacts with different positions on eIF2. This second hypothesis is more consistent with the identification of eIF2(αP) as a competitive inhibitor of eIF2B (39). In our version of this model (Fig. 10), the GCD2-GCD7-GCN3 regulatory domain forms a surface that contacts the α subunit of eIF2 in the vicinity of the phosphorylation site at Ser-51. GCD1 and GCD6 would interact with the γ subunit of eIF2 and contribute most of the residues in the active site that catalyze nucleotide exchange. The interaction between the GCD2-GCD7-GCN3 regulatory domain and the phosphorylated α subunit of eIF2 would prevent nucleotide exchange, either by distorting the catalytic center in eIF2B (Fig. 10B) or by interfering with proper positioning of the γ subunit of eIF2 in the active site.

The regulatory mutations isolated in this study could disrupt key contacts between the regulatory surface formed by GCD2, GCD7, and GCN3 and eIF2α which are required to distinguish between phosphorylated and nonphosphorylated eIF2. One possibility is that the mutations decrease the affinity of eIF2B for eIF2(αP), diminishing its effectiveness as a competitive inhibitor. We disfavor this idea for the *GCD2-L381Q* and *GCD2-K627T* mutations because >80% of the eIF2α can be phosphorylated in mutants containing these alleles (Fig. 9). If the eIF2B in *GCD2-L381Q* and *GCD2-K627TGCD2* mutants cannot utilize eIF2(αP) as a substrate, then the ability of these mutants to grow normally with more than 80% of their eIF2 phosphorylated implies that less than 20% of the wild-type eIF2 can support a high level of translation initiation. This seems unlikely unless these eIF2B mutations also increase the rate of exchange on nonphosphorylated eIF2 · GDP. We prefer the simpler explanation that mutant eIF2B complexes in the strains bearing the most effective suppressors have gained the ability to catalyze nucleotide exchange on phosphorylated eIF2. This is shown in Fig. 10C. Consistent with this model, in vitro experiments with mammalian factors have shown that eIF2(αP) · GTP can form an active ternary complex with initiator tRNA^{Met} (27), and this complex can bind to 40S ribosomal subunits (45). The ability to accept eIF2(αP) as a substrate could arise from an altered interaction between the GCD2-GCD7-GCN3 regulatory surface and the α subunit of eIF2 that allows proper positioning of the phosphorylated substrate in the active site. Alternatively, the regulatory mutations could prevent interactions between eIF2B subunits needed to distort the active site when eIF2(αP) is bound (Fig. 10C).

The model in Fig. 10 has two critical structural features: (i) the use of homologous regions in GCD2, GCD7, and GCN3 to form a single regulatory domain with contacts between these three subunits in eIF2B and (ii) the use of other homologous segments in these proteins to form a surface which interacts with eIF2α in regions surrounding the phosphorylation site. While we propose (item ii) that homologous segments in GCD2, GCD7, and GCN3 are involved in the interaction with eIF2α, it appears that each protein utilizes a distinct set of amino acid positions to carry out its regulatory function. Whereas substitutions at the identical positions in *GCN3-S293R* and *GCD7-S359G* both overcome the inhibitory effects of eIF2(αP) on eIF2B, the corresponding substitution in *gcd2-S638R* causes a reduction in eIF2B function. Similarly, the *GCD7-P291S* allele suppresses the effects of eIF2(αP), but the *gcd2-P502S* substitution at the corresponding position makes eIF2B hypersensitive to eIF2(αP). These findings can be explained by proposing that GCD2, GCD7, and GCN3 employ overlapping, but nonidentical, amino acid positions in their homologous domains to make unique contacts with different locations in eIF2α. It is interesting that similar structural features have been identified by X-ray crystallography of antigen-antibody complexes. The light and heavy chains of the antibody molecule interact with one another in regions of sequence similarity between the two chains, and each chain makes specific contacts with the antigen across a continuous surface at the interface between the antigen and antibody (14, 26). In addition, the recognition of phosphoserine at position 51 in eIF2α by eIF2B is a process that may be similar to the recognition of phosphotyrosine by SH2 domains (32, 34).

PKR has been implicated as a tumor suppressor based on the fact that expression of catalytically defective forms of PKR, which inhibit the endogenous enzyme, transformed NIH 3T3 cells and led to tumor formation in nude mice (28, 31). It is unclear whether the tumor suppressor activity of PKR involves down-regulation of eIF2 function, as PKR is also involved in transcriptional regulation of NF-κB (29). Support for the idea that inhibition of eIF2 recycling is critical for the tumor suppressor activity of PKR was provided by showing that overexpression of the nonphosphorylatable Ala-51 mutant of eIF2α duplicated the phenotypes of expressing catalytically defective PKR (18). However, these results could be explained by an

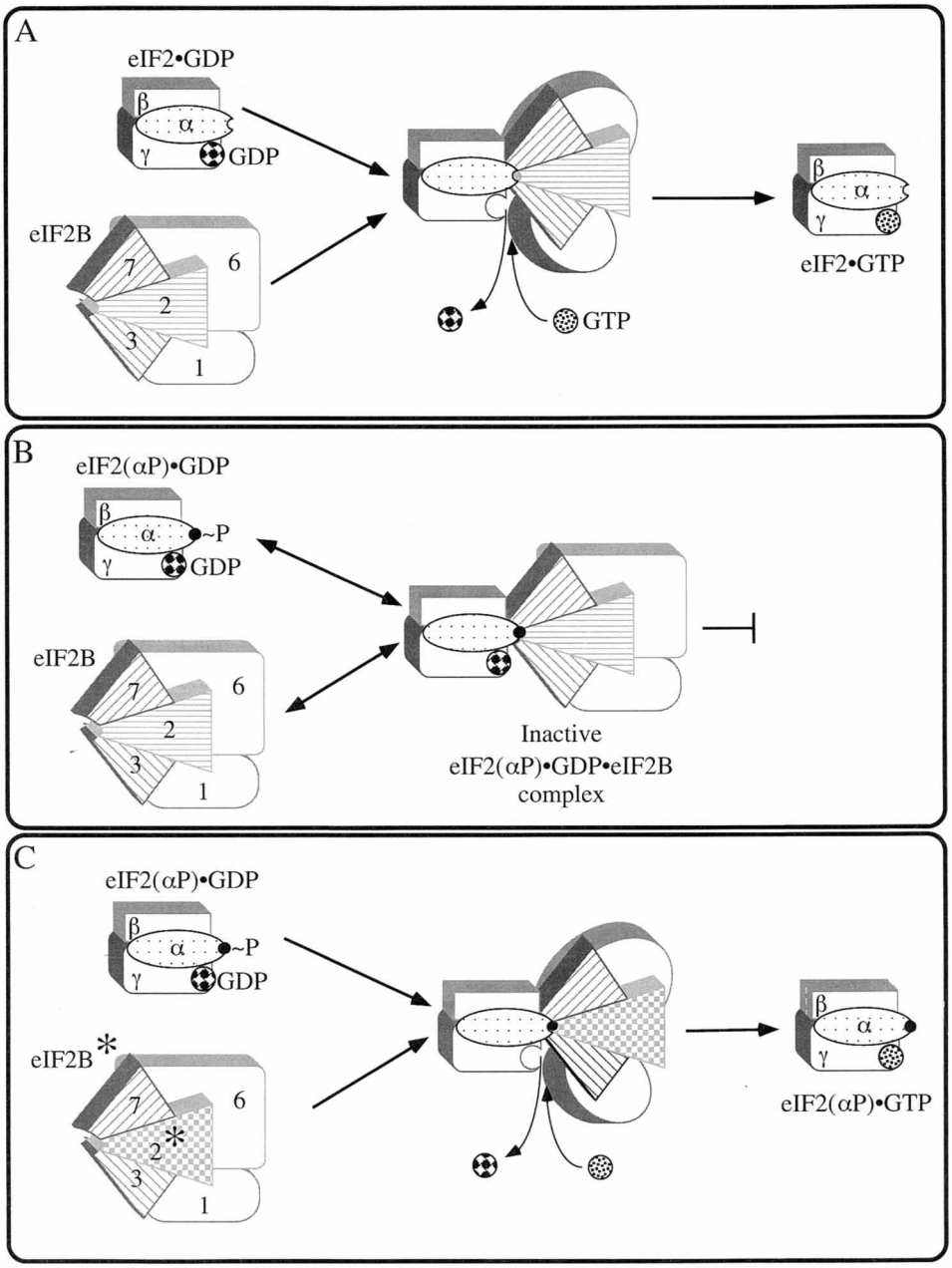

FIG. 10. Model for interactions between eIF2 and eIF2B during guanine nucleotide exchange and inhibition by phosphorylated eIF2. eIF2 (composed of three subunits, α, β, and γ) is shown interacting with eIF2B (subunits labelled 7, 2, 3, 6, and 1 representing GCD7, GCD2, GCN3, GCD6, and GCD1, respectively). The α subunit of eIF2 (depicted as an ellipse) contacts the regulatory domain composed of homologous eIF2B subunits GCD7, GCD2, and GCN3 (represented as similarly shaped wedges), along a single interface between the three regulatory subunits of eIF2B and the region of eIF2α around serine 51, the site of phosphorylation. The GCD1 and GCD6 subunits are depicted making additional contacts with the β and γ subunits of eIF2. (A) We propose that when the α subunit of bound eIF2 is not phosphorylated, this is recognized by the regulatory domain of eIF2B. The eIF2 · GDP · eIF2B complex undergoes a hypothetical conformational change in eIF2B (represented here as a shape change in GCD1 and GCD6) which leads to an exchange of GDP for GTP on eIF2. (B) In the presence of eIF2(αP), phosphoserine at position 51 in the bound eIF2 is detected by direct contacts made between eIF2(αP) and the eIF2B regulatory domain. These contacts prevent the conformational change in GCD1 and GCD6 required for GDP-GTP exchange on eIF2, such that eIF2(αP) · GDP is released unaltered. Biochemical experiments indicate that eIF2(αP) · GDP binds eIF2B with higher affinity than does nonphosphorylated eIF2 · GDP, suggesting that repeated binding and release of eIF2(αP) · GDP mediates competitive inhibition of guanine nucleotide exchange (39). (C) Possible mode of action of eIF2B regulatory mutants to allow guanine nucleotide exchange with phosphorylated eIF2. Mutant eIF2B (eIF2B*), shown here with a *GCD2* mutation (2*), alters the interaction between eIF2(αP) · GDP and eIF2B in a way that allows guanine nucleotide exchange to proceed.

indirect mechanism whereby overexpression of nonphosphorylatable eIF2α leads to the formation of PKR · eIF2α complexes that prevent PKR from phosphorylating other substrates. Introducing mutations in mammalian eIF2B subunits analogous to those described here for the yeast factor may produce eIF2B molecules with reduced sensitivity to eIF2(αP). This would provide an ideal test to determine whether the tumor suppressor activity described for PKR is mediated by phosphorylation of eIF2α and hence inhibition of eIF2B function.

ACKNOWLEDGMENTS

We thank Pat Romano and Chris Paddon for plasmids; Tom Dever, Sue Rider, and Pat Romano for critical reading of the manuscript; and members of our laboratory for helpful discussions.

G.D.P. was funded in part by a long-term fellowship from the European Molecular Biology Organisation.

REFERENCES

1. **Alani, E., L. Cao, and N. Kleckner.** 1987. A method for gene disruption that allows repeated use of *URA3* selection in the construction of multiply disrupted yeast strains. Genetics **116:**541–545.
2. **Altschul, S. F., W. Gish, W. Miller, E. W. Myers, and D. J. Lipman.** 1990. Basic local alignment search tool. J. Mol. Biol. **215:**403–410.
3. **Boeke, J. D., J. Trueheart, G. Natsoulis, and G. R. Fink.** 1987. 5-Fluoroorotic acid as a selective agent in yeast molecular genes. Methods Enzymol. **154:** 164–175.
4. **Boguski, M. S., and F. McCormick.** 1993. Proteins regulating Ras and its relatives. Nature **366:**643–654.
5. **Bushman, J. L., A. I. Asuru, R. L. Matts, and A. G. Hinnebusch.** 1993. Evidence that GCD6 and GCD7, translational regulators of *GCN4*, are subunits of the guanine nucleotide exchange factor for eIF-2 in *Saccharomyces cerevisiae*. Mol. Cell. Biol. **13:**1920–1932.
6. **Bushman, J. L., M. Foiani, A. M. Cigan, C. J. Paddon, and A. G. Hinnebusch.** 1993. Guanine nucleotide exchange factor for eIF-2 in yeast: genetic and biochemical analysis of interactions between essential subunits GCD2, GCD6, and GCD7 and regulatory subunit GCN3. Mol. Cell. Biol. **13:**4618–4631.
7. **Cadwell, R. C., and G. F. Joyce.** 1992. Randomization of genes by PCR mutagenesis. PCR Methods Appl. **2:**28–33.
8. **Chong, K. L., L. Feng, K. Schappert, E. Meurs, T. F. Donahue, J. D. Friesen, A. G. Hovanessian, and B. R. G. Williams.** 1992. Human p68 kinase exhibits growth suppression in yeast and homology to the translational regulator GCN2. EMBO J. **11:**1553–1562.
9. **Christianson, T. W., R. S. Sikorski, M. Dante, J. H. Shero, and P. Hieter.** 1992. Multifunctional yeast high-copy-number shuttle vectors. Gene **110:** 119–122.
10. **Cigan, A. M., J. L. Bushman, T. R. Boal, and A. G. Hinnebusch.** 1993. A protein complex of translational regulators of *GCN4* is the guanine nucleotide exchange factor for eIF-2 in yeast. Proc. Natl. Acad. Sci. USA **90:**5350–5354.
11. **Cigan, A. M., M. Foiani, E. M. Hannig, and A. G. Hinnebusch.** 1991. Complex formation by positive and negative translational regulators of *GCN4*. Mol. Cell. Biol. **11:**3217–3228.
12. **Clemens, M. J.** 1996. Protein kinases that phosphorylate eIF2 and eIF2B, and their role in eukaryotic cell translational control, p. 139–172. *In* J. W. B. Hershey, M. B. Mathews, and N. Sonenberg (ed.), Translational control. Cold Spring Harbor Laboratory Press, Cold Spring Harbor, N.Y.
13. **Craddock, B. L., N. T. Price, and C. G. Proud.** 1995. Cloning and expression of cDNAs for the β subunit of eukaryotic initiation factor-2B, the guanine nucleotide exchange factor for eukaryotic initiation factor-2. Biochem. J. **309:**1009–1014.
14. **Davies, D. R., and G. H. Cohen.** 1996. Interactions of protein antigens with antibodies. Proc. Natl. Acad. Sci. USA **93:**7–12.
15. **Dever, T. E., J. J. Chen, G. N. Barber, A. M. Cigan, L. Feng, T. F. Donahue, I. M. London, M. G. Katze, and A. G. Hinnebusch.** 1993. Mammalian eukaryotic initiation factor 2α kinases functionally substitute for GCN2 in the *GCN4* translational control mechanism of yeast. Proc. Natl. Acad. Sci. USA **90:**4616–4620.
16. **Dever, T. E., L. Feng, R. C. Wek, A. M. Cigan, T. D. Donahue, and A. G. Hinnebusch.** 1992. Phosphorylation of initiation factor 2α by protein kinase GCN2 mediates gene-specific translational control of *GCN4* in yeast. Cell **68:**585–596.
17. **Dever, T. E., W. Yang, S. Astrom, A. S. Bystrom, and A. G. Hinnebusch.** 1995. Modulation of $tRNA_i^{Met}$, eIF-2, and eIF-2B expression shows that *GCN4* translation is inversely coupled to the level of eIF-2-GTP · Met-$tRNA_i^{Met}$ ternary complexes. Mol. Cell. Biol. **15:**6351–6363.
18. **Donze, O., R. Jagus, A. E. Koromilas, J. W. B. Hershey, and N. Sonenberg.** 1995. Abrogation of translation initiation factor eIF-2 phosphorylation causes malignant transformation of NIH 3T3 cells. EMBO J. **14:**3828–3834.
19. **Hannig, E. M., and A. G. Hinnebusch.** 1988. Molecular analysis of *GCN3*, a translational activator of *GCN4*: evidence for posttranslational control of *GCN3* regulatory function. Mol. Cell. Biol. **8:**4808–4820.
20. **Harashima, S., and A. G. Hinnebusch.** 1986. Multiple *GCD* genes required for repression of *GCN4*, a transcriptional activator of amino acid biosynthetic genes in *Saccharomyces cerevisiae*. Mol. Cell. Biol. **6:**3990–3998.
21. **Hinnebusch, A. G.** 1988. Mechanisms of gene regulation in the general control of amino acid biosynthesis in *Saccharomyces cerevisiae*. Microbiol. Rev. **52:**248–273.
22. **Hinnebusch, A. G.** 1994. Translational control of *GCN4*: an *in vivo* barometer of initiation factor activity. Trends Biochem. Sci. **19:**409–414.
23. **Hinnebusch, A. G.** 1996. Translational control of *GCN4*: gene-specific regulation by phosphorylation of eIF2, p. 199–244. *In* J. W. B. Hershey, M. B. Mathews, and N. Sonenberg (ed.), Translational control. Cold Spring Harbor Laboratory Press, Cold Spring Harbor, N.Y.
24. **Hinnebusch, A. G., and G. R. Fink.** 1983. Positive regulation in the general amino acid control of *Saccharomyces cerevisiae*. Proc. Natl. Acad. Sci. USA **80:**5374–5378.
25. **Ito, H., Y. Fukada, K. Murata, and A. Kimura.** 1983. Transformation of intact yeast cells treated with alkali cations. J. Bacteriol. **153:**163–168.
26. **Jones, S., and J. M. Thornton.** 1996. Principles of protein-protein interactions. Proc. Natl. Acad. Sci. USA **93:**13–20.
27. **Konieczny, A., and B. Safer.** 1983. Purification of the eukaryotic initiation factor 2-eukaryotic initiation factor 2B complex and characterization of its guanine nucleotide exchange activity during protein synthesis initiation. J. Biol. Chem. **258:**3402–3408.
28. **Koromilas, A. E., S. Roy, G. N. Barber, M. G. Katze, and N. Sonenberg.** 1992. Malignant transformation by a mutant of the IFN-inducible dsRNA-dependent protein kinase. Science **257:**1685–1689.
29. **Kumar, A., J. Haque, J. Lacoste, J. Hiscott, and B. R. G. Williams.** 1994. Double-stranded RNA-dependent protein kinase activates transcription factor NF-κB by phosphorylating IκB. Proc. Natl. Acad. Sci. USA **91:**6288–6292.
30. **Merrick, W. C.** 1992. Mechanism and regulation of eukaryotic protein synthesis. Microbiol. Rev. **56:**291–315.
31. **Meurs, E. F., J. Galabru, G. N. Barber, M. G. Katze, and A. G. Hovanessian.** 1993. Tumor suppressor function of the interferon-induced double-stranded RNA-activated protein kinase. Proc. Natl. Acad. Sci. USA **90:**232–236.
32. **Moran, M. F., C. A. Koch, D. Anderson, C. Ellis, L. England, G. S. Martin, and T. Pawson.** 1990. Src homology region 2 domains direct protein-protein interactions in signal transduction. Proc. Natl. Acad. Sci. USA **87:**8622–8626.

32a. **Paddon, C., and A. G. Hinnebusch.** Unpublished observations.

33. **Paddon, C. J., and A. G. Hinnebusch.** 1989. *gcd12* mutations are *gcn3*-dependent alleles of *GCD2*, a negative regulator of *GCN4* in the general amino acid control of *Saccharomyces cerevisiae*. Genetics **122:**543–550.
34. **Pawson, T., and G. D. Gish.** 1992. SH2 and SH3 domains: from structure to function. Cell **71:**359–362.
35. **Ramirez, M., R. C. Wek, C. R. Vazquez de Aldana, B. M. Jackson, B. Freeman, and A. G. Hinnebusch.** 1992. Mutations activating the yeast eIF-2α kinase GCN2: isolation of alleles altering the domain related to histidyl-tRNA synthetases. Mol. Cell Biol. **12:**5801–5815.

35a. **Romano, P., and A. G. Hinnebusch.** Unpublished observations.

36. **Romano, P. R., S. R. Green, G. N. Barber, M. B. Mathews, and A. G. Hinnebusch.** 1995. Structural requirements for double-stranded RNA binding, dimerization, and activation of the human eIF-2α kinase DAI in *Saccharomyces cerevisiae*. Mol. Cell. Biol. **15:**365–378.
37. **Rose, M., P. Novick, J. Thomas, D. Botstein, and G. R. Fink.** 1987. A *Saccharomyces cerevisiae* plasmid bank based on a centromere-containing shuttle vector. Gene **60:**237–243.
38. **Rose, M. D., and J. R. Broach.** 1991. Cloning genes by complementation in yeast. Methods Enzymol. **194:**195–230.
39. **Rowlands, A. G., R. Panniers, and E. C. Henshaw.** 1988. The catalytic mechanism of guanine nucleotide exchange factor action and competitive inhibition by phosphorylated eukaryotic initiation factor 2. J. Biol. Chem. **263:**5526–5533.
40. **Sambrook, J., E. F. Fritsch, and T. Maniatis.** 1989. Molecular cloning: a laboratory manual, 2nd ed. Cold Spring Harbor Laboratory, Cold Spring Harbor, N.Y.
41. **Sherman, F., G. R. Fink, and C. W. Lawrence.** 1974. Methods in yeast genetics. Cold Spring Harbor Laboratory, Cold Spring Harbor, N.Y.
42. **Sikorski, R. S., and P. Hieter.** 1989. A system of shuttle vectors and yeast host strains designed for efficient manipulation of DNA in *Saccharomyces cerevisiae*. Genetics **122:**19–27.
43. **Southern, E.** 1975. Detection of specific sequences among DNA fragments separated by gel electrophoresis. J. Mol. Biol. **98:**503–517.
44. **Trachsel, H.** 1996. Binding of initiator methionyl-tRNA to ribosomes, p. 113–138. *In* J. W. B. Hershey, M. B. Mathews, and N. Sonenberg (ed.), Translational control. Cold Spring Harbor Laboratory Press, Cold Spring Harbor, N.Y.
45. **Trachsel, H., and T. Staehelin.** 1978. Binding and release of eukaryotic initiation factor eIF-2 and GTP during protein synthesis initiation. Proc. Natl. Acad. Sci. USA **75:**204–208.
46. **Vazquez de Aldana, C. R., T. E. Dever, and A. G. Hinnebusch.** 1993. Mutations in the α subunit of eukaryotic translation initiation factor 2 (eIF-2α) that overcome the inhibitory effects of eIF-2α phosphorylation on translation initiation. Proc. Natl. Acad. Sci. USA **90:**7215–7219.
47. **Vazquez de Aldana, C. R., and A. G. Hinnebusch.** 1994. Mutations in the GCD7 subunit of yeast guanine nucleotide exchange factor eIF-2B overcome the inhibitory effects of phosphorylated eIF-2 on translation initiation. Mol. Cell. Biol. **14:**3208–3222.
48. **Wek, R. C.** 1994. eIF-2 kinases: regulators of general and gene-specific translation initiation. Trends Biochem. Sci. **19:**481–486.
49. **Wek, R. C., J. F. Cannon, T. E. Dever, and A. G. Hinnebusch.** 1992. Trun-

cated protein phosphatase GLC7 restores translational activation of *GCN4* expression in yeast mutants defective for the eIF-2α kinase GCN2. Mol. Cell. Biol. **12:**5700–5710.

50. **Wek, R. C., B. M. Jackson, and A. G. Hinnebusch.** 1989. Juxtaposition of domains homologous to protein kinases and histidyl-tRNA synthetases in GCN2 protein suggests a mechanism for coupling *GCN4* expression to amino acid availability. Proc. Natl. Acad. Sci. USA **86:**4579–4583.
51. **Wek, R. C., M. Ramirez, B. M. Jackson, and A. G. Hinnebusch.** 1990. Identification of positive-acting domains in GCN2 protein kinase required for translational activation of *GCN4* expression. Mol. Cell. Biol. **10:**2820–2831.
52. **Yang, W., and A. G. Hinnebusch.** 1996. Identification of a regulatory subcomplex in the guanine nucleotide exchange factor eIF2B that mediates inhibition by phosphorylated eIF2. Mol. Cell. Biol. **16:**6603–6616.